1   **ESTABLISHED AND EMERGING TECHNIQUES FOR CHARACTERISING THE FORMATION, STRUCTURE**

2   **AND PERFORMANCE OF CALCIFIED STRUCTURES UNDER OCEAN ACIDIFICATION**

3   SUSAN C. FITZER[1]‡*, VERA BIN SAN CHAN[2, 3, 4]‡, YUAN MENG[4], KENMANI CHANDRA RAJAN[4],

4   SUZUKI MICHIO[5], CHRISTELLE NOT[6], TAKASHI TOYOFUKU[7], LAURA FALKENBERG[8, 9], MARIA

5   BRYNE[10, 11], BEN P. HARVEY[12], PIERRE DE WIT[13], MAGGIE CUSACK[14], K. S. GAO[15], PAUL TAYLOR[16],

6   SAM DUPONT[17], JASON HALL-SPENCER[18], V. THIYAGARAJAN[4]*

7   [1]*Institute of Aquaculture, Faculty of Natural Sciences, University of Stirling, Pathfoot Building,*

8   *Stirling, FK9 4LA, UK*

9   [2]*Department of Biological Sciences, Clemson University, Clemson, SC 29634 USA*

10 [3] *Ifremer, Physiologie Fonctionnelle des Organismes Marins UMR 6539 LEMAR*

11 *(CNRS/UBO/IRD/Ifremer) Technopole Iroise - CS 10070 29280 Plouzane, France.*

12 [4]*The Swire Institute of Marine Sciences and School of Biological Sciences, The University of Hong*

13 *Kong, Pokfulam, Hong Kong, China.*

14 [5]*Graduate School of Agricultural and Life Sciences, The University of Tokyo, Tokyo, Japan.*

15 [6]*Department of Earth Sciences, The University of Hong Kong, Hong Kong, China*

16 [7]*Japan Agency of Marine Earth Science and Technology JAMSTEC, Department of Marine*

17 *Biodiversity Research BioDive, Yokosuka, Kanagawa, Japan*

18 [8]*Norwegian Institute for Water Research NIVA, NIVA Region West, Thormøhlensgate 53 D*

19 *5006 Bergen, Norway*

20 [9]*Simon F.S. Li Marine Science Laboratory, School of Life Sciences, The Chinese University of Hong*

21 *Kong, Hong Kong*

22 [10]*School of Medical Sciences, University of Sydney, Sydney, New South Wales, Australia*

23 [11]*School of Life and Environmental Sciences, University of Sydney, Sydney, New South Wales,*

24 *Australia*

25   [12]Shimoda Marine Research Center, University of Tsukuba, 5-10-1 Shimoda Shizuoka 415-0025,

26   Japan

27   [13]Department of Marine Sciences, University of Gothenburg, 45296 Stromstad, Sweden

28   [14]Division of Biological & Environmental Sciences, Faculty of Natural Sciences, University of

29   Stirling, Cottrell Building, Stirling, FK9 4LA, UK

30   [15]The State Key Laboratory of Marine Environmental Science, Xiamen University, Xiamen, China.

31   [16]Department of Earth Sciences, Natural History Museum, Cromwell Rd, London SW7 5BD, UK.

32   [17]Department of Biological and Environmental Sciences, University of Gothenburg, 45178

33   Fiskebackskil, Sweden.

34   [18]School of Biological and Marine Sciences, Plymouth University, Plymouth PL4 8AA, Devon, UK

35   ‡ shared first-authorship

36   *corresponding authors:

37   Susan C. Fitzer

38   e-mail: susan.fitzer@stir.ac.uk

39   V. Thiyagarajan

40   e-mail: rajan@hku.hk

41   Ocean acidification (OA) is the decline in seawater pH and saturation levels of calcium carbonate

42   minerals that has led to concerns for calcifying organisms such as corals, oysters and mussels because

43   of the adverse effects of OA on their biomineralisation, shells and skeletons. A range of cellular biology,

44   geochemistry and materials science approaches have been used to explore biomineralisation. These

45   techniques have revealed that responses to seawater acidification can be highly variable among species,

46   yet the underlying mechanisms remain largely unresolved. To assess the large-scale impacts of global

47   OA, researchers will need to apply a range of tools developed across disciplines, many of which are

48 emerging and have not yet been used in this context. This review outlines techniques that could be

49 applied to study OA-induced alterations in the mechanisms of biomineralisation and their ultimate

50 effects on shells and skeletons. We illustrate how to characterise, quantify and monitor the process of

51 biomineralisation in the context of global climate change and OA. We highlight the basic principles as

52 well as the advantages and disadvantages of established, emerging, and future techniques for OA

53 researchers. A combination of these techniques will enable a holistic approach and better understanding

54 of the potential impact of OA on biomineralisation and consequences for marine calcifiers and

55 associated ecosystems.

Introduction

57 The precipitation of minerals such as calcium carbonate ($CaCO_3$) for shells and skeletons using

58 dissolved carbonate and calcium ions is commonly called 'biomineralisation' (Doney et al. 2009).

59 Marine organisms have been producing calcium carbonate biominerals since the Precambrian and the

60 resultant rich fossil record provides insight into the evolution of intricate, orderly and often beautiful

61 structures (Wilkinson 1979). The composition of biominerals varies among taxa and, as the production

62 of shell materials is dependent on the availability of mineral ion resources and on physiological

63 conditions at the site of calcification (Wilbur 1964), mineral composition can reveal how organisms

64 have interacted with environmental conditions over geological time to the present day.

65 Atmospheric CO_2 levels have increased at a faster rate during the Anthropocene than in any previous

66 time in Earth's history causing a rapid decline in seawater pH and lowering the amount of calcium

67 carbonate minerals (Orr et al. 2005).

68 Since concerns about OA were first highlighted it has become apparent that CO_2-driven acidification

69 can lead to skeletal abnormalities and slower growth in many marine calcifiers (Hofmann et al. 2008,

70 Vézina and Hoegh-Guldberg 2008, Wittmann and Pörtner 2013). Aragonite, calcite, vaterite

71 (Wehrmeister et al. 2011), and amorphous calcium carbonate which is an important precursor of

72 crystalline carbonate minerals (Addadi et al. 2003), are phases of $CaCO_3$ whose production may be

73 modified by OA. Organisms can be affected by OA as they need to maintain conditions that are

74   chemically suitable for the process of calcification (supersaturated with calcium $[Ca^{2+}]$ and carbonate

75     $[CO_3^{2-}]$) or for preventing dissolution (saturation state $\Omega > 1$). Calcite is less susceptible to dissolution

76   at lower pH values than aragonite, unless it contains high levels of magnesium (Ries et al. 2009, Chan

77   et al. 2012). Production of any form of $CaCO_3$ can be energetically expensive (Comeau et al. 2017a)

78   and so the impact of OA on the production and maintenance of $CaCO_3$ structures are modulated by

79   energy acquisition (Melzner et al. 2011) and may be due to by CO_2-driven organism hypercapnia (Byrne

80   et al. 2013).

81   To capture fully the impact of OA on biomineralisation, several key questions should be addressed.

82   These include questions regarding the direct impact of OA on the process of biomineralisation itself

83   and also about the functional consequences of these changes on shells and skeletons. Resolving these

84   issues requires multidisciplinary research ranging from '–omics' to cell culture, from physiological

85   mechanisms to ecology, and from materials science to crystallography. The complexity of the task is

86   reflected in the plethora of techniques that have been used to investigate biomineralization under OA

87   conditions, including buoyant weight, total alkalinity anomaly, total calcium content, annual estension,

88   calcein labelling and the use of radio isotopes (Table 1). This diversity of approaches allows

89   investigators to tackle different questions related to the impact of OA on the process of

90   biomineralisation, although there is a need to understand how different techniques compare when

91   measuring similar processes (Schoepf et al. 2017). The selection and refinement of a technique is

92   dependent upon scientific question and practical aspects related to the study question, experimental

93   design and biological models (Figure 1).
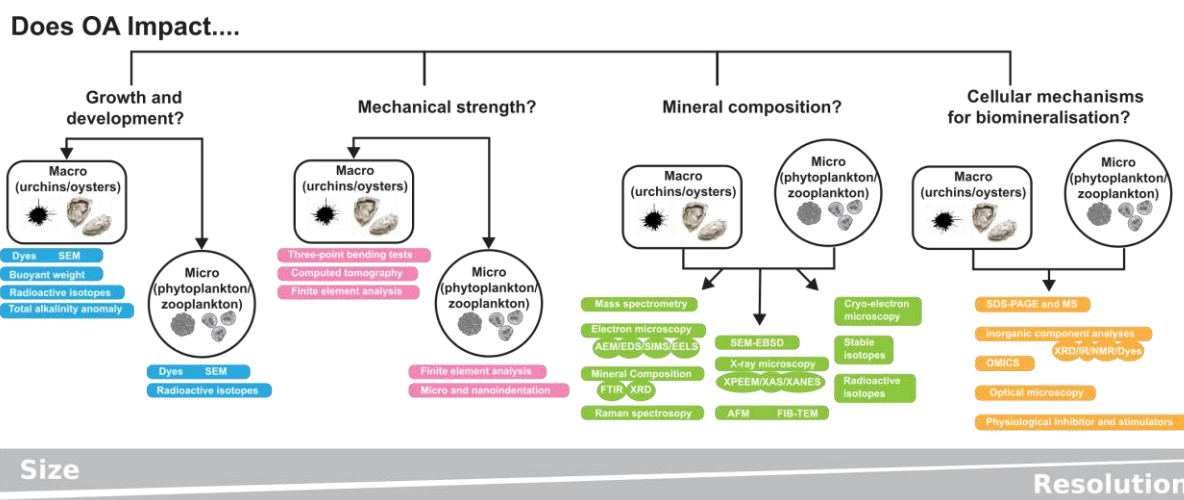
94

95 **Figure 1. A schematic representation of analytical methods studying whole animal growth and**

96 **development (in blue), mechanical strength (in pink), mineral composition (in green), and cellular**

97 **mechanisms of biomineralisation (in orange) that enables the answering of various level of**

98 **questions. These techniques can be strategically applied to macrobiota (e.g. urchin or oysters) or**

99 **microbiota (e.g. phytoplankton or zooplankton). From left to right, the figure shows the techniques**

100 **applicable to smaller scale samples with increasing resolution. At a lower resolution, macrobiota**

101 **can be measured in terms of various shell growth and development parameters (in blue) and**

102 **mechanical properties, while some approach has more limitations with microbiota. At a high**

103 **resolution, microbiota and macrobiota can be studied for their shell structure (in green) and cellular**

104 **mechanisms for biomineralisation (in orange).**

105

106 Here we review an array of techniques used to explore the consequences of rising global CO_2 levels on

107 biomineralisation in marine organisms. We organize the techniques by categorizing the biological or

108 mineralogical parameters of interest. We evaluate their advantages and disadvantages so that future

109 work can more effectively measure the effects of OA on biomineralisation . We also highlight recent

110 advances in the study of the effects of ocean acidification on biomineralisation and how

111 interdisciplinary collaboration can advance the field.

112   *Growth and development*

113   When evaluating the impact of OA on biomineralisation, it is important to discriminate between

114   methods measuring gross and net calcareous shell growth as the product of biomineralisation (Figure

115   2). The term 'gross calcification' refers to the biologically controlled process of $CaCO_3$ production

116   through the formation of $CaCO_3$ minerals from a super saturated solution ($CaCO_3$ precipitation). In

117   contrast, the term 'net calcification' is the net effect of gross calcification and dissolution (Cyronak et

118   al. 2016). $CaCO_3$ dissolution or decalcification is the dissolution of $CaCO_3$ minerals in an under

119   saturated solution. These processes combine to influence net calcification; for example, the upregulation

120   in gross calcification rates of the limpet *Patella caerulea* helps to counteract higher shell dissolution

121   rates (Rodolfo-Metalpa et al. 2011).
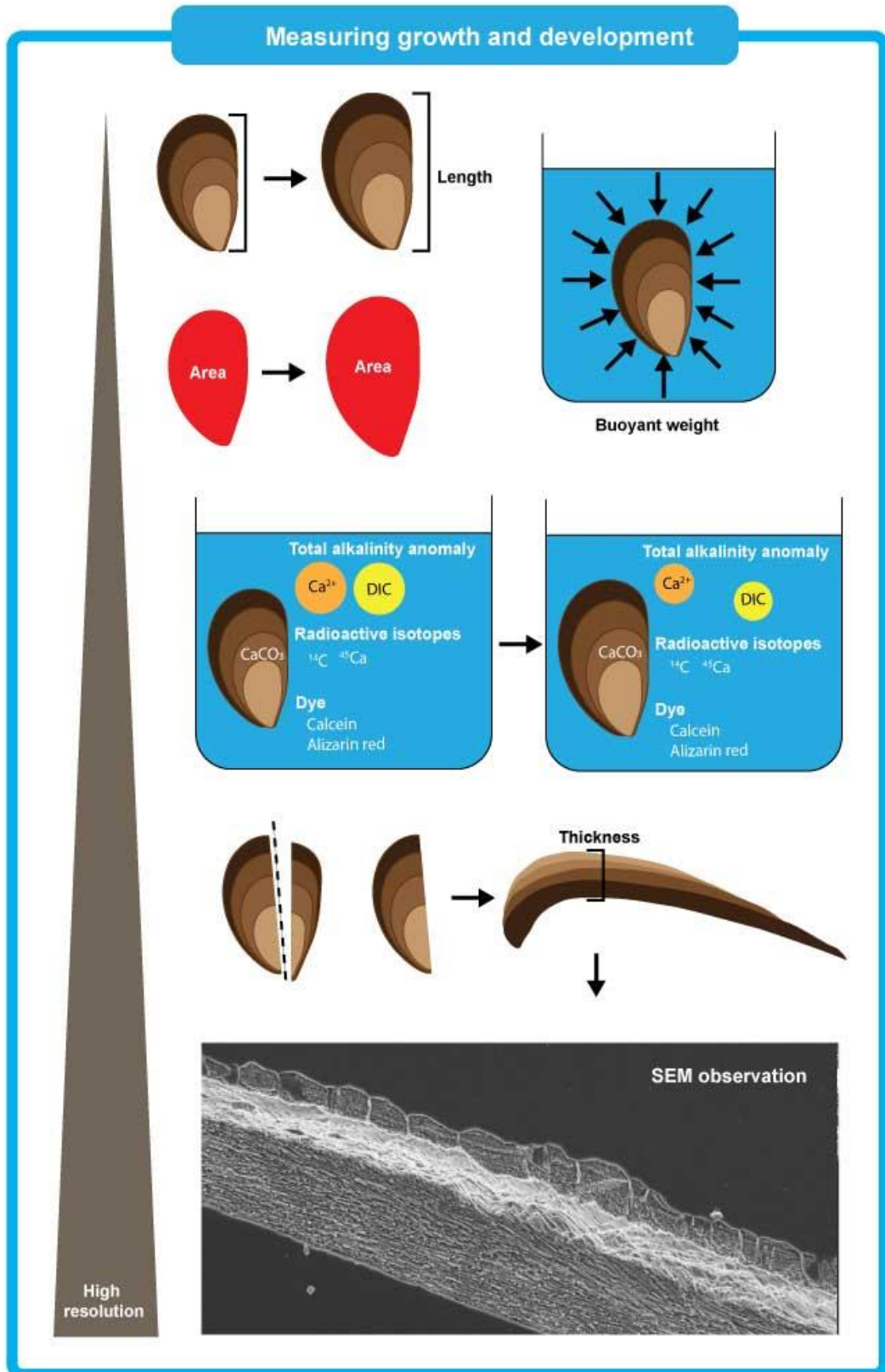
123 **Figure 2. Schematic representation of techniques for measuring growth and development in**

124 **biomineralising organisms. The tapering bar on the left indicates the changing level of resolution for**

125 **each technique. From top to bottom, growth and development can be measured on whole shells**

126 **and skeletons using techniques such as length and buoyant weight measurements. More sensitive**

127 **techniques are represented in the middle for the use of dyes, radioactive isotopes and total**

128 **alkalinity anomaly technique. At the bottom of the figure, sectional surface of a shell at higher**

129 **resolution can be visualized and thickness can be measured using techniques such as SEM**

130 **microscopy.**

131

132 *Dyes*

133 A range of chemical dyes (e.g. alizarin red, calcein) are used to mark shells or exoskeletons to assess

134 growth over time and have been used in OA studies to determine the impact on calcification in corals,

135 coralline algae and bivalves (Rodolfo-Metalpa et al. 2011, Dickinson et al. 2012a, Tambutté et al. 2012,

136 Bradassi et al. 2013, Venn et al. 2013, Fitzer et al. 2014b, Fitzer et al. 2015b). Calcein labelling is often

137 preferable because calcein was found better incorporated into foraminiferan calcite and emitted

138 fluorescence more strongly than the other markers such as Alizarin complexone, oxytetracycline, and

139 xylenol orange (Bernhard et al. 2004). Calcein has been applied in OA research to assess coralline algal,

140 coral and mollusc growth during experiments (Dickinson et al. 2012b, Bradassi et al. 2013, Venn et al.

141 2013, Fitzer et al. 2014b, Fitzer et al. 2015b). The techniques are low cost, less invasive as compared

142 to sacrificial shell sampling and the results are readily comparable.

143 *SEM*

144 Abnormalities and morphology can be assessed by optical microscopy. However, scanning electron

145 microscopy (SEM) is required for high resolution characterisation of biomaterial microstructures and

146 has been used to show modified skeletal phenotypes in a range of species grown under OA conditions

147 (Riebesell et al. 2000, Orr et al. 2005, Iglesias-Rodriguez et al. 2008, Lombardi et al. 2015). The

148   advantage of this approach include the ability to assess shape and malformation in net growth, while

149   the disadvantages include higher costs and an extended preparation time.

150   When evaluating net shell growth as the overall product of biomineralisation, one of the simplest and

151   most widely used methods to approximate net calcification is shell and exoskeleton length, as it is both

152   non-invasive low-cost. However, this approach can fail to reveal impacts on gross and net calcification

153   not expressed in the overall structure of the skeleton. For example, OA can cause skeletal malformations

154   which can only be identified by microscopy (Langdon et al. 2000, Reynaud et al. 2003, Langdon and

155   Atkinson 2005, Gazeau et al. 2007, Cooper et al. 2008, Jokiel et al. 2008, Ries et al. 2009). This can be

156   partly addressed by including morphometric parameters to resolve shapes, and thickness, for example

157   using 3-dimensional measurements generated from computed tomography (Rühl et al. 2017). It is

158   therefore important to consider the net growth of the whole shell or skeleton.

159   Skeletal growth assessed as annual extension rate (cm^2 yr^{-1}) is commonly used to determine growth

160   rates of calcareous red algae and corals (Marsh 1970), with recent research applying photogrammetric

161   methods based on digital photography and advanced image processing techniques for non-destructive

162   measurements of area and volume (Mackenzie et al. 2014, Norzagaray-López et al. 2017). Densitometry

163   using X-rays (Table 2) assesses the density of calcified structures (Carricart-Ganivet and Barnes 2007)

164   and has been used to identify growth bands and to calculate growth rates of individuals or colonies

165   (Cooper et al. 2008).

Buoyant weight

167   To monitor changes in mineral content, buoyant weight determined by immersion is frequently used

168   (Davies 1989, Herler and Dirnwöber 2011). Correction for seawater salinity and temperature variation

169   between measurements is necessary (Fang et al. 2013). The buoyant weight technique is non-invasive

170   (Molina et al. 2005) and remains one of the most common techniques to determine net calcification rate

171   in OA studies, especially in corals (Herler and Dirnwöber 2011). Such an approach has shown that an

172   array of temperate corals *Oculina arbuscula*, pencil urchins *Eucidaris tribuloides*, hard clams

173   *Mercenaria mercenaria*, conchs *Strombus alatus*, serpulid worms *Hydroides crucigera*, periwinkles

174   *Littorina littorea*, bay scallops *Argopecten irradians*, oysters *Crassostrea virginica*, whelks *Urosalpinx*

175   *cinerea*, and soft clams *Mya arenaria* show mixed responses to CO_2-induced acidification, thereby

176   highlighting the complexity of biomineralisation responses (Ries et al. 2009).

177   *Radioactive isotopes*

178   Naturally occurring radioactive isotopes can be used to measure growth by spiking organisms with a

179   radiotracer (Sabatier et al. 2012). Liquid scintillation counting is used to amplify the signal and

180   quantify the amount or rate of ^{45}Ca being incorporated into the biomineral structure (Rodolfo-Metalpa

181   et al. 2011, Rodolfo-Metalpa et al. 2015). ^{45}C is a non-natural radioactive isotope, therefore any changes

182   in ^{45}Ca quantity represents shell material accretion or loss by the calcification process that occurs during

183   the experiment and prior calcification is not taken in account (Furla et al. 2000). Similarly, synthetic

184   radioactive ^{14}C isotopes enable the measurement of carbon flux related to photosynthesis and

185   calcification (Guo et al. 2009, Li et al. 2015). The ^{45}Ca technique has been used in OA research to

186   determine the impact of increasing pCO$_2$ levels on cold-water corals, suggesting that calcification is not

187   disrupted under OA (Rodolfo-Metalpa et al. 2015). Gross calcification rates have been quantified using

188   ^{45}Ca in corals, limpets, mussels, foraminifera, coccolithophores and oyster larvae (McEnery and Lee

189   1970, Erez 1978, Satoh et al. 2009, Rodolfo-Metalpa et al. 2011, Rodolfo-Metalpa et al. 2015, Frieder

190   et al. 2016). In contrast, ^{14}C has mainly been applied in unicellular organisms such as coccolithophores

191   (Paasche 1963, Nimer and Merrett 1993, Gao et al. 2009), foraminifera (ter Kuile et al. 1989), and

192   diatoms (Li et al. 2015). Advantages include the improved spatial resolution, taking into account

193   material accretion during the incubation period. However, a major disadvantage of this technique is the

194   destructive nature of sampling unlike other techniques such as buoyant weight to determine calcification

195   rates.

196   *Total alkalinity anomaly technique*

197   Net calcification rate can be measured by determining the amount of $CaCO_3$ taken up by an organism

198   (Gazeau et al. 2007). When an organism precipitates a mole of $CaCO_3$ it takes up two moles of HCO_3^-,

199   thereby reducing the alkalinity of the surrounding seawater over the incubation period (Langdon et al.

200 2000, Langdon and Atkinson 2005, Gazeau et al. 2007). The total alkalinity anomaly technique has

201 been used as an alternative to the buoyant weight method to determine net calcification rates in a range

202 of calcifying organisms including corals, mussels and oysters (Langdon et al. 2000, Langdon and

203 Atkinson 2005, Gazeau et al. 2007). A recent study recommends that the technique is more suitable for

204 shorter term (e.g. day/night) incubations whereas the buoyant weight method is suitable for longer term

205 studies when resources are limited (Schoepf et al. 2017). Less frequently, calcium content has been

206 determined directly using mass spectrometry as a proxy for calcification (Wood et al. 2008). Both the

207 total alkalinity anomaly and the buoyant weight techniques are low cost and take into account skeleton

208 malformations, however there is variability between incubation methods. Promisingly, there is

209 agreement in the results obtained from the different methods, with the major trend of a reduction in net

210 biomineralisation under OA shown by both techniques (Langdon et al. 2000, Langdon and Atkinson

211 2005, Gazeau et al. 2007).

212 **Mechanical tests - Protective function or ability to survive**

213 OA impacts the gross and net calcification in many marine calcifiers, and therefore it would be expected

214 that OA would similarly impact the function of the shell or skeleton. Mechanical properties of

215 shells/skeletons can be quantified by two parameters: a) hardness (resistance to irreversible

216 deformation) and b) compressive strength (force needed to induce cracking). These parameters can be

217 used to evaluate the functional impacts of changes in biomineralisation under OA. For example, changes

218 in these parameters have implications on the vulnerability of reef-forming species and associated

219 ecosystems, as well as consequences for predator-prey interactions (Fu et al. 2016).

220 *Three-point bending tests*

221 As a classical, simplistic and low cost approach to examine mechanical features of brittle biomineral

222 structures, three-point bending tests measure the flexural strength and modulus and commonly used to

223 define material properties in its ability to resist bending. Three-point bending tests have been applied to

224 measure the stiffness of the ambital plates in sea urchins grown in OA and found that there can be no

225 significant impact on the protective function of the exoskeleton (Collard et al. 2016). Purpose-made

11

226   devices consisting of two supportive beams with appropriate span length and a loading beam can be

227   built according to the specific morphology of the biomineral sample (Guidetti and Mori 2005, Asnaghi

228   et al. 2013). These tests provide relevant information to the protective function of the shell or

229   exoskeleton. The flexural response to a three-point bending test device mimics the deformation response

230   to predatory attack by fish (Guidetti and Mori 2005). This exoskeleton robustness test was applied in

231   the OA study of a sea urchin, and revealed increased $p\mathrm{CO}_2$ reduced the defense of a sea urchin to the

232   predator (Asnaghi et al. 2013). If samples are to be directly compared, it is essential to first standardize

233   the thickness and sectional area of the test material, which requires additional preparation time to ensure

234   the biomineral samples are cut into a standard size. The three-point bending tests have the advantage of

235   being able to measure the whole structure mechanical response; disadvantages are that it can be time

236   consuming as purpose-made devices may be required for unusually shaped shell structures.

237

238   *Computed tomography*

239   Computed tomography (CT) and micro-computed tomography (Micro-CT) are powerful, non-

240   destructive techniques to evaluate biomineralised structures. Micro-CT allows 3D visualisation of X-

241   ray image series generated by scanning with axial rotation in small steps. This method enables

242   examination of internal structural features at fine spatial resolution (Li et al. 2016). A micro-CT dataset

243   allows a variety of quantifiable measurements, including thickness in terms of pixel distance, volume

244   in terms of voxel counts and density in terms of brightness of each pixel at higher resolution compared

245   to CT (Fantazzini et al. 2015, Tambutté et al. 2015, Chatzinikolaou et al. 2017).

246   With these 3D geometric morphometrics and measurements, the growth rate, density and morphological

247   changes due to OA can be investigated. Micro-CT has been applied in OA studies on gastropods

248   (Chatzinikolaou et al. 2017), tubeworms (Li et al. 2014, Li et al. 2016), and shrimp (deVries et al. 2016)

249   to infer changes in the protective function of the exoskeletons. 3D model visualisation also enables the

250   analysis of density distribution to understand the engineering of calcareous structures. Consequently,

251   the presence of structurally vulnerable regions can be identified. Micro-CT analysis has been used in

252   OA to determine the survival of coral through protective exoskeleton function (Tambutté et al. 2015).

253   Exoskeleton porosity often represents shell protective function. In particular, intertidal gastropods

254   *Nassarius nitidus* and *Columbella rustica* exhibited density reduction in acidified conditions

255   (Chatzinikolaou et al. 2017) while coral skeletons also showed an increased porosity at lower pH

256   through micro-CT (Fantazzini et al. 2015, Tambutté et al. 2015).

257   The spatial resolution of most medical micro-CT is sufficient to provide a good measurement for large

258   calcifiers, and typically have a resolution of 15 - 1000 μm per pixel. As a consequence, however,

259   observation of marine plankton and larvae remains as a challenge. Another limitation of micro-CT is

260   the detection sensitivity which can generate false negatives through thin minerals where regions may

261   appear as empty space in the 3D reconstruction. Therefore, it is important to verify the representative

262   morphology by combining micro-CT with an SEM approach. All density measurements should be

263   calibrated with a standard material which has a known bone mineral density (BMD, $g.cm^{-3}$) in terms of

264   calcium hydroxyapatite and its corresponding pixel intensity for each scan (Li et al. 2014). Since there

265   are no commercially available standards for calcium carbonate calibration, density measurements are

266   relative and has limited comparability with other studies.

267   *Finite element analysis*

268   The field of engineering and computational simulation can be applied creatively to understand structural

269   impacts to biominerals caused by OA. In a simulation, any weakness in the architecture is highlighted

270   and the loading capacity can be calculated from the shape and empirical data (Li et al. 2016). Therefore,

271   the application of structural analysis can be performed when shapes and mechanical properties of the

272   biological mineral are both known, providing a holistic picture of how well each calcified material

273   functions as the protective or supportive structure.

274   The most widely applied numerical tool for computational simulation is finite element analysis (FEA)

275   (Li et al. 2014; Li et al. 2016). To solve a problem using FEA, the problem is divided into smaller and

276   simpler parts which are called finite elements. By assembling the solution of all finite elements

277   mathematically, a total approximate solution of the large problem can be obtained. FEA enables the

278   mechanical behaviours of complex biomineralised structures to be investigated accurately. The FEA

279 can include the different experimental mechanical properties, such as elasticities of different

280 components of the shell structure, as well as simulate the effects of loading, for example the crushing

281 forces associated with a predator attack.

282 With the diverse calcareous structures being produced by marine organisms, FEA can be applied to

283 assess changes in mechanical performances due to morphological changes. For example, FEA has been

284 applied to understand the mechanical response of a tubeworm under OA combined with low salinity

285 and warming treatments. This enabled the identification of the most vulnerable region of the tube and

286 the highest risk of fracture failure under predatory attack (Li et al. 2014, Li et al. 2016). This

287 demonstrates that FEA can be developed as biologically accurate model to determine the impact of OA

288 on the protective function of calcareous shells and exoskeletons. Beside its advantage, FE models

289 especially when it is 2-D simplified (Ragazzola et al. 2012), often fail to account for heterogeneity,

290 malformation and shape changes. In addition, 3-D models are complex and requires advanced

291 computational efforts (Melbourne et al. 2015).

292 *Micro- and nanoindentation*

293 Biominerals are composed of mineral crystals and an organic matrix framework. As a result, biogenic

294 calcite has been reported to be 50-70% harder than geological calcite (Kunitake et al. 2012, Kunitake

295 et al. 2013). Due to the high heterogeneity in morphology, structure and composition of mineralized

296 shells and exoskeletons, hardness has been widely used as a comparable evaluation of mechanical

297 properties (Beniash et al. 2010, Dickinson et al. 2012a, Fitzer et al. 2015b).

298 The strength of biomineralised structures can be characterised by a crushing or compressive test where

299 machine applies and reads compressive force- versus displacement. The entire structure of specimens

300 can be used to mimic a predatory attack (Byrne et al. 2014). However, biomineralised structures are

301 typically not homogenous and using a single point allows a better mechanical understanding of the shell

302 property.
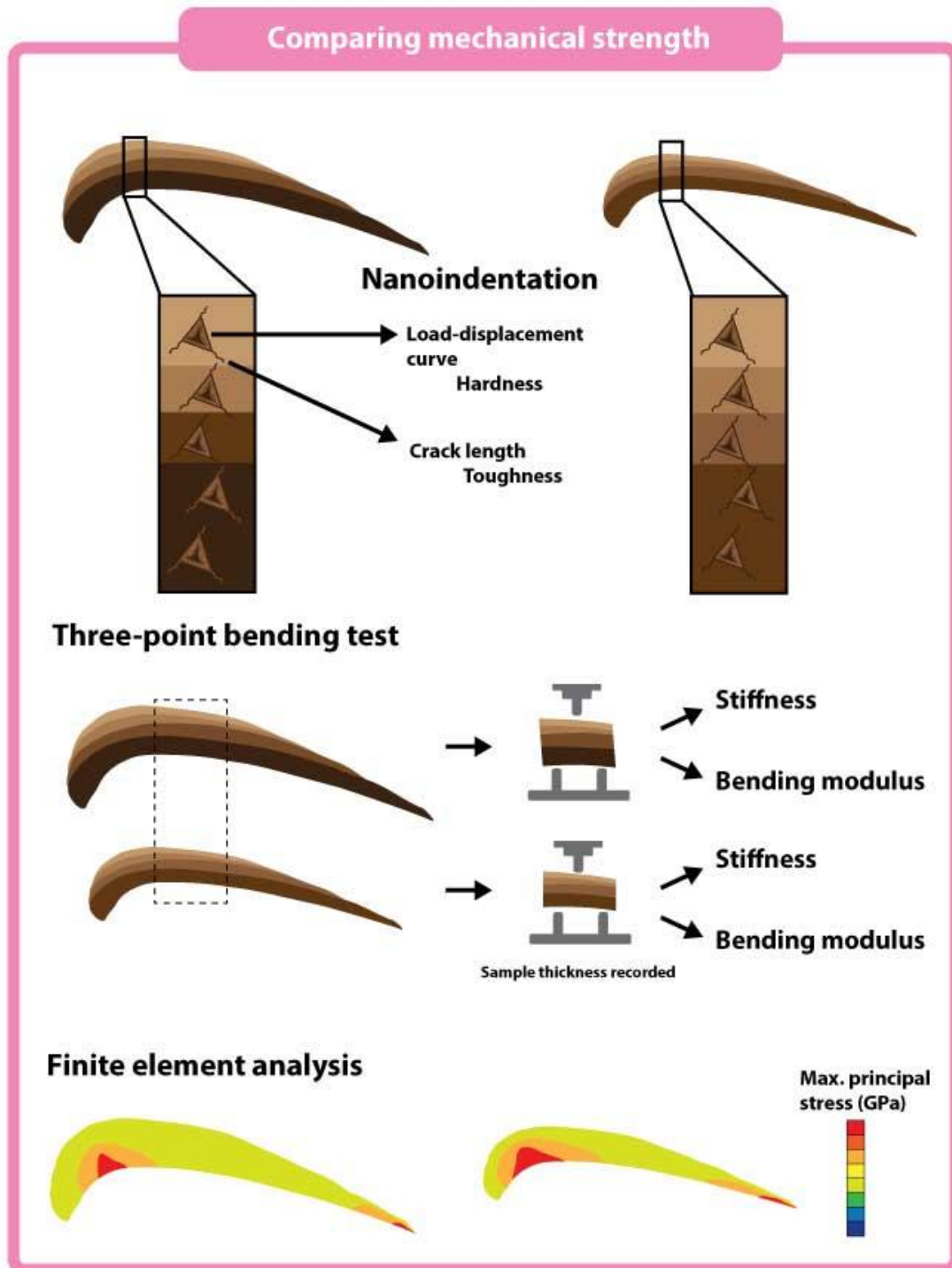
Figure 3. Schematic representation of techniques to compare mechanical properties in biomineralizing organisms. Nanoindentation and 3-point bending are two highlighted techniques for assessing mechanical properties including hardness, elasticity, fracture toughness and stiffness

307 **of biominerals. Micro and nanoindentation in combination of computed tomography and finite**

308 **element analysis project the impact of OA on mechanical properties of shells and skeletons during**

309 **predatory attacks.**

310

311 Two main methods can be used to understand the impact of OA on shell mechanical properties (Figure

312 3): 1) microhardness tests can measure Vickers hardness numbers (HV) determined by the ratio of the

313 force applied by the indenter and the surface area of the final indent (Beniash et al. 2010, Dickinson et

314 al. 2012a); and 2) nanoindentation which can measure the hardness and elasticity in a single indent.

315 With the development of a depth-sensing indenter, the hardness and elastic modulus (a measure of

316 stiffness) in units of pascals (Pa) from each indentation can be obtained from the loading-unloading

317 curve by using the Oliver-Pharr model (Oliver and Pharr 1992). This method enables the measurement

318 of shell hardness and has been used to address how the protective function of several mollusc species

319 grown under experimental OA might be affected (Beniash et al. 2010, Dickinson et al. 2012a, Fitzer et

320 al. 2015b). The results indicate no significant impact on microhardness in clams (Beniash et al. 2010)

321 and oysters (Dickinson et al. 2012a) but an increase in microhardness in mussels (Fitzer et al. 2015c).

322 The advantage of nanoindentation is its precision at the nanometre scale. Nanoindentation enables

323 spatial refinement where the mechanical properties profile can be examined (Li et al. 2014). At finer

324 spatial resolution, mechanical features can be associated with the different textures of the mineral

325 (Goffredo et al. 2014). The influence of OA can be reflected in different mineralised layers or structures

326 of the marine invertebrate shell. Nanoindentation enables substantial refinement, for example, the

327 hardness and modulus of the tubeworm from the exterior to the interior were mapped by

328 nanoindentation in order to address questions about the protective function of the structure (Li et al.

329 2014, Fitzer et al. 2015b). The mechanical properties of the exterior to the interior portion of the tube

330 were shown to decrease under OA compared to the middle portion of a tubeworm (Li et al. 2014).

331 Researchers can analyse the same polished sample using SEM, allowing correlation between structural

332 alteration and mechanical performance. This has been done for mussels (Fitzer et al. 2015b) and

16

333   tubeworms (Chan et al. 2012, Li et al. 2014) grown in OA for extended periods of time showing that

334   OA-induced structural alteration may lead to deteriorations in mechanical performance. Both hardness

335   tests have the disadvantage of requiring a highly polished sample surface (Perez-Huerta and Cusack

336   2009) and sample preparation can be both time-consuming and challenging (Milano et al. 2016).

337   In addition to hardness, the dimensions of the cracks generated around the indent can be used to

338   determine the fracture toughness combined with the elasticity of the material as shown for bivalves

339   grown under OA conditions (Beniash et al. 2010, Dickinson et al. 2012a, Fitzer et al. 2015b). By

340   measuring the lengths of cracks, the plane-strain fracture toughness (KIC) can be calculated (Lawn et

341   al. 1980, Anstis et al. 1981). However, it is difficult to define the local and bulk fracture behaviours by

342   this technique, which makes it problematical to determine the accuracy of the fracture toughness values

343   given by indentation (Kruzic et al. 2009). This technique has enabled the determination of the impact

344   of OA on shell protective function: the fracture toughness of oyster shells and mussel shells was reduced

345   (as measured by microhardness tests), which confirmed that the calcite shell became more brittle in OA

346   conditions (Beniash et al. 2010, Dickinson et al. 2012a, Fitzer et al. 2015b).

347   **Mineral composition - Biomineralisation mechanisms to enable shell growth**

348   Trace elements present in seawater are incorporated within the shell structure of calcifying organisms

349   and several empirical relationships have been observed between the trace element to calcium ratio and

350   environmental parameters of the surrounding water. For example, the Mg/Ca ratio of a shell is positively

351   correlated with the temperature of the surrounding water (Nürnberg et al. 1996, Dwyer et al. 2002,

352   Pérez-Huerta et al. 2008, Kamenos et al. 2013). Based on empirical and experimental calibration,

353   several element to calcium ratios have been observed to reflect the environmental condition. Trace

354   element to calcium ratios and particularly Mg/Ca and Sr/Ca have been widely used to understand the

355   biomineralisation process (but noted that biological activity can influence the elemental composition in

356   the mineral rather than recording the environmental conditions, Weiner and Dove 2003). For example,

357   OA has been shown to affect trace element to calcium ratios in corals (Sinclair 2005), foraminifera

358   (Elderfield et al. 1996, Keul et al. 2013, Not et al. 2018), ostracods (Dwyer et al. 2013), and tubeworms

359   (Chan et al. 2015b), but not sea urchins (Byrne et al 2014). For sea urchins grown under OA and

360   warming from the juvenile to the adult stage, the Mg/Ca was not affected by OA but, as expected, was

361   altered by temperature (Byrne et al. 2014). When exposed to OA, Mg/Ca increased in vermetid shells,

362   suggesting a dissolution of aragonite and increase in calcite (Chan et al. 2012, Milazzo et al. 2014).

363   Milazzo et al. (2014) applied inductively coupled plasma optical emission spectrometry (ICP-OES)

364   techniques to understand impacts of OA on calcification as growth and suggested that under OA shell

365   dissolution will occur with the potential to impact survival through weakened shell protection.

366   *Mass spectrometry*

367   A variety of methods are available to measure the elemental ratios of a biological mineral. Basically,

368   calcifying organisms can be measured in a solid phase using techniques such as X-ray fluorescence

369   (XRF) or laser ablation (LA) or in dissolved phase after dilution using a range of inductively coupled

370   plasma spectrometry. Since trace elements are measured within the mineral, several cleaning steps are

371   required to remove organic matter and potential lithogenic contamination (Martin and Lea 2002).

372   Typically, analysis of a dissolved sample by inductively coupled plasma (ICP) spectrometry requires

373   the preparation of the shell or skeleton sample by acid digestion, fusion, or ash drying. Techniques for

374   solution analyses include, ICP- optical emission spectrometry (OES), ICP- atomic emission

375   spectroscopy (AES), ICP-mass spectrometry (MS), and multiple collector (MC) ICP-MS. The

376   differences between these ICP spectrometry techniques are the increase of precision of the analyses, the

377   higher resolution and therefore lower detection limits of elements up to isotopic measurement with MC-

378   ICP-MS, whereas the disadvantages are the cost and maintenance of the equipment.

379   *Electron microscopy AEM/ EDS/ SIMS/ EELS*

380   Spatial information of elemental distribution in the mineral provides valuable information to predict

381   mechanical properties. Solid-sampling methods have been developed for ICP analysis for this purpose.

382   Electro-thermal-vaporisation (ETV) and laser ablation (LA) are applied to generate vapour for

383   characterisation. In combination with ICP-OES or ICP-MS, these techniques are suitable for analysis

384   of a solid sample (Limbeck et al. 2017). However, LA-ICP-MS only provides resolution of > 5 µm,

385   while secondary ion mass spectrometry (SIMS) distinguishes sub-micrometre resolution (Becker et al.

386   2010). Although SIMS has a sensitive detection level of 1 ppm, the technique is not directly quantitative

387   due to its dependence on a solid-state chemical standard, and the nonlinear and highly variable nature

388   of the ionisation process of different elements in SIMS (Williams 1985). In addition, SIMS can be used

389   to obtain depth profiles of mineral composition of shells (Jeffree et al. 1995). All of these methods have

390   an advantage of giving spatial information on the elemental distribution, the differences lie in the

391   resolution between ICP-MS, ICP-OES and SIMS. ICP-OES is already applied using acid digestion of

392   collected individuals for determination of elemental ratios (Milazzo et al. 2014). The application of

393   SIMS to OA research would enable the analysis of much smaller samples and to examine the response

394   of individual calcifying organisms in terms of growth and survival (Eichner et al. 2017).

395   The spatial detection of trace elements on a bulk material surface can be achieved through electron

396   microscopy (Müller et al. 2011). Analytical electron microscopy (AEM) with energy dispersive X-ray

397   spectrometry (EDS) and wavelength-dispersive X-ray spectroscopy (WDS) provides data at the

398   nanometre scale (Newbury 1998). EDS offers an advantage of greater specimen area than the high

399   resolution method of electron energy loss spectrometry (EELS), which also requires a 10 nm thick

400   specimen to be prepared. Therefore, EDS is a more efficient and accessible AEM approach for OA

401   research. Notably, detection levels of AEM-EDS are around 1000 ppm, EELS 10 ppm and structured

402   illumination microscopy (SIMS) 1 ppm. EDS and WDS both enable the microanalysis of biominerals

403   and provide additional spatial information of the elemental profile. The cost of EDS is considerably

404   lower than WDS and has a high acquisition speed. In comparison, the spectral resolution of WDS is

405   superior to that of EDS. These techniques have been applied to address the question of whether OA

406   would have an impact on the calcification of shrimp and tubeworm skeletons, in order to understand

407   the impact on exoskeleton critical function including protective defense against predators (Chan et al.

408   2012, Taylor et al. 2015). EDS was employed to determine magnesium content in the exoskeleton of

409   shrimps grown under OA with the finding that increased calcium content with lowered pH resulted in

410   a greater Mg/Ca ratio (Taylor et al. 2015). Mg/Ca as an environmental indicator of calcite has been

411   suggested to increase as aragonite saturation decreases (Chan et al. 2012).

412   Taken together, there has been significant growth in a number of techniques available for quantifying

413   elements present in liquid and solid materials. Some of the surface techniques such as LA-ICP-MS, and

414   other analytical electron microscopy (AEM) techniques, such as SIMS, AEM-EDS and AEM-EELS,

19

415   have different resolutions and sample preparation requirements which should be considered in the

416   context of experimental objectives. The recent development of MS analytic methods for bioimaging

417   opens opportunities to investigate mineralising tissues at the biomolecule level (Becker et al. 2010).

418   Complementing optical and electron microscopy techniques as discussed in the following section, these

419   tools will enable a better understanding of the mechanism of OA impacts on the processes involved in

420   the production of biominerals. However, these techniques at present have the disadvantages of requiring

421   sample specific standards for calibration, time consuming sample preparation, observation confined to

422   a tiny area of interest and the destructive nature of sample analysis.

423

424   *Mineral composition analyses by FTIR and XRD*

425   Mineral composition characterisation techniques target the comparison of mineral phases, elemental

426   ratios and amorphous calcium carbonate to clarify the intricate process of biomineralisation (Figure 4).

427   In the context of OA, it is important to understand the process of biomineralisation mechanisms to

428   appreciate how continued growth will be possible under future environmental change.

429
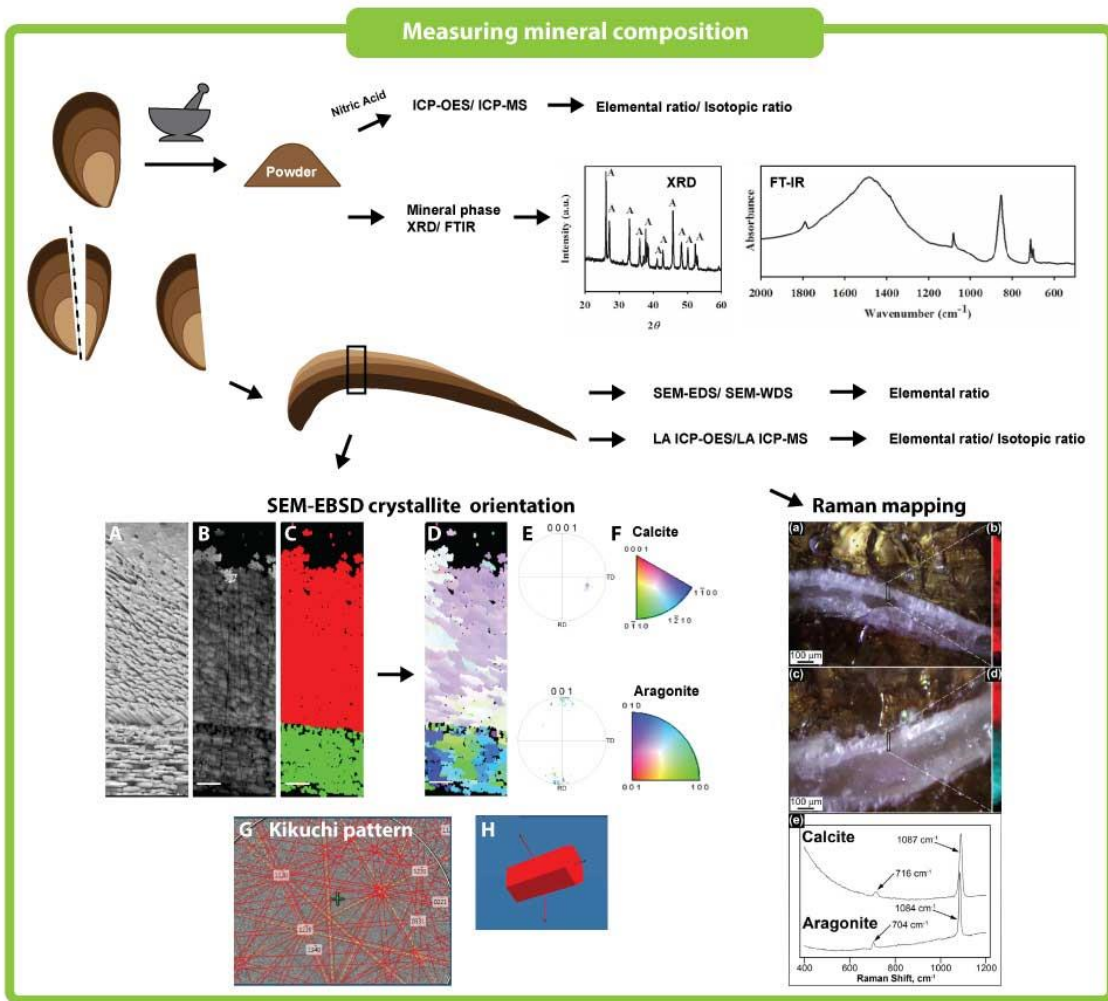
Figure 4. Schematic representation of highlighted techniques for characterizing mineral composition in biomineralising organisms. Shell power samples are digested prior to mass spectrometry characterisation, e.g. ICR-OES/ICP-MS, for determining elemental ratio or isotopic ratio. Sectional surface of the shell are inspected for elemental ratio mapping using electron microscopy techniques such as SEM-EDS or SEM-WDS; or using mass spectrometry approaches by LA-ICP-MS or LA-ICP-OES. Additionally, a sample of shell powder provides mineral phase indentification using FTIR or XRD, figures modified from Chan et al., (2012). SEM-EBSD, SEM-WDS and Raman spectroscopy are highlighted as techniques to determine the mineral composition and crystallographic orientation in a mussel shell to determine the impacts on shell growth under OA as an alternative to techniques such as ICP-OES or ICP-MS to determine elemental or isotope ratios in biominerals. SEM-EBSD figure

440　**data taken from Fitzer et al., (2014a). Secondary electron images of the crystal structure from an**

441　**etched (a) and polished (b) sample, the mineral composition can be seen in the phase map where**

442　**calcite is shown in red and aragonite in green (c). The crystallographic orientation map (d),**

443　**corresponding pole figures (e) and colour keys (f) are indicated for calcite and aragonite. EBSD uses**

444　**Kikuchi patterns to identify the mineral phase (g) and the crystallographic orientation (h). Raman**

445　**mapping figure modified from Chan et al., (2015b). Raman microscopy has been used to provide**

446　**photomicrographs of younger (a)　and older regions　(c), of a juvenile tubeworm,　phase　maps**

447　**indicate regions of aragonite only (b) and aragonite and calcite (d) in the tube. A Raman spectra**

448　**(e) of aragonite and calcite has been measured in the same specimen (c).**

449

450　Fourier-transform infrared (FTIR) spectra can be used to determine the relative quantity of amorphous

451　calcium carbonate from an intensity ratio ($I_{max}\nu_2/I_{max}\nu_4$) between the absorption bands. The major

452　disadvantage of the FTIR approach is its semi-quantitative nature; results can only be compared within

453　the same experimental dataset. This method has been adopted in OA research on a marine tube worm

454　where amorphous calcium carbonate content was found to be higher at low pH (Chan et al. 2012, Leung

455　et al. 2017). Chan et al. (2012) suggest that this result indicates the presence of an active shell repair

456　mechanism when animals are counteracting shell weakening by OA. The advantage of FTIR is that it

457　takes as little as 1 mg of mineral sample and so may be applied to larval specimens.

458　The ratio of calcite and aragonite content, that has implications for the vulnerability of shells and

459　skeletons to OA, can be quantified by X-ray diffraction (XRD). This is an advantage over FTIR, but

460　XRD has its own drawback, i.e. the loss of spatial resolution due to the need for powdered samples.

461　XRD approach has been used to assess shell or exoskeleton growth under OA. Unless containing large

462　amounts of Mg, calcite is considered to be less susceptible to dissolution at lower pH values than

463　aragonite (Ries et al. 2009, Chan et al. 2012). OA relevant changes in thickness of the calcite and

464　aragonite layers was first noted in mussels transplanted into low-pH environments (Hahn et al. 2012).

465　Calcite: aragonite ratios have been shown to change under OA, leading to a thinner and more vulnerable

466   aragonite layer in mussel shells (Fitzer et al. 2015a). The shell thickness index in comparison to the

467   measured thickness of the aragonite or calcite layers uses the thickness, the length, height and dry mass

468   of the shell and is considered to produce a lower measurement error compared to direct measurement

469   (Freeman and Byers 2006, Naddafi and Rudstam 2014, Fitzer et al. 2015a). The shell thickness index,

470   in comparison to XRD, has an advantage of being non-destructuive to the sample, but a disavantage

471   with a loss in spatial resolution.

472   *Raman spectroscopy*

473   Raman spectroscopy is a non-destructive technique that enables molecular bonds and mineralogical

474   information to be precisely characterised at a submicron resolution. By illuminating a sample with a

475   monochromatic laser beam, a Raman spectrum is generated that contains unique peaks that are

476   diagnostic of mineral polymorphs due to their characteristic Raman shifts (Eisenstein et al. 2016).

477   Structural components, such as calcite, aragonite and collagen, have been identified and mapped with

478   resolution as fine as 1 µm (Eisenstein et al. 2016, Taylor et al. 2016). Advantages of Raman

479   spectroscopy over other spectroscopic methods, such as FTIR, include the improved spatial resolution

480   and the direct relevance of this method for biomineralisation, as well as the potential to examine samples

481   in their native state (Eisenstein et al. 2016, Von Euw et al. 2017). This technique is considered a

482   complementary method to FTIR, and is perhaps more suitable for OA studies. Raman microscope

483   imaging has been applied to OA research to identify the mineral composition and polymorphic forms

484   to assess rates of calcification under increasing pCO_2 in coralline algae and limpets (Kamenos et al.

485   2013, Langer et al. 2014). For instance, Raman mapping of the shells of limpets from a CO_2 vent

486   demonstrated that the polymorph distribution pattern is maintained despite living at low pH (Langer et

487   al. 2014). In coralline algae, although calcification continues under OA, Raman has identified disorder

488   in the molecular position of the carbonate ions which suggests a weakened skeletal structure (Kamenos

489   et al. 2013). These applications were used to assess exoskeleton structural weaknesses which can impact

490   the protective function of the calcified structures under OA.

491   *SEM-EBSD*

23

492   Electron backscatter diffraction (EBSD) is widely used to determine the crystallographic orientation of

493   biogenic minerals. EBSD provides additional information to precursory SEM imaging of shell

494   dissolution or exoskeletal microstructure as it allows for the examination of microstructure at the

495   individual crystal level. The technique identifies Kikuchi patterns (Kikuchi 1928, Nishikawa and

496   Kikuchi 1928) as scattered electrons are reflected as per Bragg's law from the crystal lattice onto a

497   phosphorus screen. It was first used to observe the impact of OA on the shell ultrastructure of the mussel

498   *Mytilus galloprovincialis* (Hahn et al. 2012) and was further applied across a broad range of species,

499   including an argonaut (Wolfe et al. 2013) and corals (Fitzer et al., 2014b; Hennige et al., 2015). The

500   effects on crystalline structure identified using this technique in OA research have been used to address

501   the question of how changes in seawater environment can impact the orderly arrangement of shell or

502   exoskeleton structures which has an implication to the animal's ability to survive.

503

504   *X-ray microscopy XPEEM – XAS and XANES*

505   An alternative emerging technique for determining the mineral composition of marine skeletons is high-

506   spatial resolution synchrotron X-ray photo emission electron microscopy (XPEEM) combined with X-

507   ray absorption spectroscopy (XAS) (Fitzer et al. 2016). The benefits of the XPEEM and XAS over SEM

508   is the high level of spatial resolution, and the fact that it can detect without the need for an energy filter

509   by measuring the secondary electrons yield as a function of photon energy. This technique can be

510   applied alongside electron backscatter diffraction (EBSD) to identify mineral phases throughout the

511   shell structure (Fitzer et al. 2016). XANES and XPEEM techniques use the principles of X-ray

512   absorption fine structure (XAFS) which interpret the scattering of photo-electrons emitted from an

513   absorbing atom in a structure when excited by high energy photons (Politi et al. 2008, Fitzer et al. 2016).

514   XANES has been used as a tool to examine the phase transformation mechanisms of amorphous calcium

515   carbonate into calcite particularly in sea urchin larval spicules (Politi et al. 2006, Politi et al. 2008, Gong

516   et al. 2012). Recently, XPEEM combined with XAS has been used as a tool to examine amorphous

517   calcium carbonate in mussels reared under OA conditions (Fitzer et al. 2016) showing more induced

518   amorphous calcium carbonate with less crystallographic control over shell formation. This technique

519   was applied to address the question of OA impact on biomineralisation and shell repair to determine

520   the protective function of the shell under changing environments (Fitzer et al. 2016). The technique

521   requires the embedding and fine-polishing of samples, similar to SEM-EBSD preparation (Politi et al.

522   2008, Perez-Huerta and Cusack 2009, Fitzer et al. 2016). XANES and XPEEM have the advantage of

523   providing high spatial resolution to locate amorphous calcium carbonate embedded within the shell

524   structure when applied in combination with SEM techniques (Politi et al. 2008). Disadvantages include

525   the high instrumentation cost and lengthy sample preparation time.

526   *AFM*

527   Atomic force microscopy (AFM) provides atomic resolution analysis of material properties. As a type

528   of scanning probe microscopy, AFM scans and interacts with a sample directly using a tip that is

529   connected to a cantilever spring. The vertical deflection and the force-distance curve are recorded by a

530   piezoelectric translator (Butt et al. 2005). In tapping mode, AFM generates fine topographical images

531   with nanometre resolution. The time-dependent relationship between applied pressure (stress) and

532   deformation (strain) represents viscoelastic properties (Butt et al. 1995) enabling the measurement of

533   local mechanical properties.

534   Easy sample preparation and high resolution are the major advantages of using AFM over conventional

535   microscopy methods (Butt et al. 1995). The typically small interacting surface for AFM must be smooth

536   and homogeneous requiring polished and etched surfaces similar to EBSD sample preparation (Dalbeck

537   et al. 2011). Therefore, AFM complements the observations of SEM-EBSD analysis which can provide

538   high resolution textural data to OA studies (Dalbeck et al. 2011). AFM performed in the presence of an

539   electrolyte solution is possible (Butt et al. 1995), therefore, enabling better biological relevance. In order

540   to obtain comparable regions of interest, correlative SEM or light microscopy data are often helpful to

541   effectively navigate at AFM resolution (Sikes et al. 2000). AFM has yet to be applied to determine the

542   impact of OA on biomineralisation. Once applied, this technique will provide a correlation with EBSD

543   data to address the question of biomineralisation mechanisms in shell growth and hence survival.

544   *FIB-TEM*

545   The finest biological observation have been via transmission electron microscopy (TEM), providing

546   resolutions of nanometres down to below an ångström (Nellist et al. 2004) exceeding 'super-resolution'

547   microscopy. In addition, TEM is an important characterisation tool that collects X-ray diffraction with

548   a micrograph enabling subcellular features and location of crystals to be analysed together. A

549   nanofabrication technique using the focused ion beam (FIB) system has emerged as a powerful tool for

550   precise TEM specimen preparation, where milling and cutting of a sample is performed inside an SEM

551   or scanning ion microscopy (SIM) (Titze and Genoud 2016). This preparation approach overcomes

552   technical challenges of manual preparation of ultrathin TEM sections, with the localisation of the region

553   of interest, and reduces the risks of sample loss (Chan et al. 2017).

554   Suzuki et al. (2011) revealed the details of five microstructures in the limpet shell using FIB-TEM. The

555   FIB technique was used to separate each microstructure in cross section to determine crystal

556   morphology and orientation. The FIB technique is powerful in handling tiny larval or juvenile shells

557   (Yokoo et al. 2011, Chan et al. 2015a, Chan et al. 2017), and reduces costs of analysis time for TEM

558   on samples with poor orientation or an unfocussed area of interest. FIB-TEM ensures a consistent

559   cutting angle at the nanoscale, so providing comparable observation of a larger number of experimental

560   samples.

561   Depending on institutional resources, fine spatial resolution, long-hour procedures performed using

562   FIB-TEM can be costly in a centralised facility. In summary, FIB-TEM is currently a qualitative

563   observational method, but it has potential to be applied in a more quantitative setting.

564   *Cryo-electron microscopy*

565   In cryo-electron microscopy, biological samples can be visualised by a freeze fracture process which is

566   achieved by rapid freezing of fixed tissue samples by vitrification (Alfredsson 2005). A hydrated sample

567   that is close to the native state can be observed in high resolution without the requirement of destructive

568   conventional preparation procedures for SEM and TEM (Levi-Kalisman et al. 2001, Khalifa et al. 2016,

569   Thompson et al. 2016). Electron microscopy also enables X-ray diffraction characterisation essential

570   for identification of minerals. Ice from humidity in the environment can contaminate the sample,

571   therefore, samples must be prepared after vitrification (Thompson et al. 2016). Technical disadvantages

572   associated with cryo- methods include the need for stabilising detergents for structure (Singh and

573   Sigworth 2015) which, in addition to its high cost, will make the application of this technique

574   challenging for large scale OA experiments.

575   *Stable isotopes*

576   Biogenic stable isotopes have been used extensively to reconstruct the paleaoclimates, in terms of

577   temperature, pH and salinity (Lear et al. 2000, Parkinson et al. 2005, Ghosh et al. 2006, McConnaughey

578   and Gillikin 2008, Martin et al. 2016, Stewart et al. 2016). They can also be used to understand

579   biomineralisation mechanisms of ion transport at the site of calcification (Furla et al. 2000, Rae et al.

580   2011, Allen et al. 2012, Allison et al. 2014). The detection of Mg, Sr, and Ca, the detection of the

581   isotopes, $\delta^{13}C$, $\delta^{18}O$, ^{10}B and $\delta^{11}B$ requires acid digestion prior to mass spectrometry analyses (Krief et

582   al. 2010). Here, we list some of the target isotopes that have promise for OA research.

583   Quantification of isotopic elements can be applied to detect the consequence of stress on calcification

584   pathways (Rae et al. 2011, Allison et al. 2014, Stewart et al. 2016). Brachiopods, in particular, form

585   their exoskeletons in good isotopic equilibrium with the seawater (Parkinson et al. 2005). Since pH is

586   dependent on two boron species: boric acid ($B(OH)_3$) and the borate ion ($B(OH)_4^-$) (Hemming and

587   Hanson 1992, Stewart et al. 2016, Zhang et al. 2017), the species of boron isotopes found in shells

588   represents the dissolved inorganic carbon (DIC) chemistry of the calcification fluid (Allison et al. 2014).

589   Stable isotope techniques have been applied in OA research to understand the mechanisms of

590   biomineralisation, specifically, whether material is laid down under control by the organism irrespective

591   of the seawater isotopes (Krief et al. 2010). For example, seawater pH impacts the skeletal $\delta^{13}C$ and δ

592   ^{18}O in corals, but there is an offset in the $\delta^{11}B$ between the calcified material and that of seawater

593   suggesting control of biomineralisation by ion-transport enzymes (Krief et al. 2010). This technique

594   addresses the question of calcification mechanism change under OA and whether there is a reduced

595   metabolic incorporation of isotopes through enzyme control, hence reduced growth and survival under

596   OA. The influence of carbonate ion concentration on $\delta^{13}C$ and $\delta^{18}O$ is still being explored, particularly

597   in foraminifera (Spero et al. 1997).

598   Isotopic approaches have the disadvantage of requiring a relatively large amount (~2 mg) of biogenic

599   calcium carbonate powder. Sample preparation with micro-milling is time-consuming and can be

600   technically challenging, especially when investigating different polymorphs and seasonal growth bands

601   in smaller specimens (Stewart et al. 2016). Advances in stable isotope techniques will consist of

602   improved ways of separating organics from biominerals, micro milling samples for biomineral powder,

603   and laser ablation methods that increase spatial resolution of measurements (Fietzke et al. 2010, Wall

604   et al. 2016).

605   *Radioactive isotopes*

606   In addition to using ^{45}Ca for estimation of calcification, radioactive isotopes can also contribute to a

607   mechanistic understanding of the calcification process. Furla et al. (2000) used a double radioactive

608   isotope experimental design (H^{14}CO$_3$ and ^{45}Ca) to show inorganic carbon transport. Comprehensive

609   measurement of both the DIC species and Ca for calcification was accomplished in terms of net

610   radioactivity by ^{14}Ca and ^{45}Ca (Furla et al. 2000). These data also unraveled the carbonate concentrating

611   mechanisms within coral cells (Furla et al. 2000).

612   The use of radioactive isotopes (^{45}Ca, ^{14}C) is specific and sensitive to experimental conditions.

613   Moreover, the maintenance of radioactive substances can be challenging. Before adopting the use of

614   radioactive isotopes within an experimental culture, a protocol must be optimised to adequately label

615   specimens and avoid contamination. Therefore, even though the approach is quite well-established in

616   environmental geochemistry (Parkinson et al. 2005, Ghosh et al. 2006, McConnaughey and Gillikin

617   2008), disadvantages of requiring continual radioactive tracer application and the destructive nature of

618   the sample digestion by acid means that it has yet to be applied more widely in OA studies (Furla et al.

619   2000).

620   **Cellular biomineralisation mechanisms**

621   The processes by which organisms control the substrate for calcification are complex and can occur

622   internally within tissues, or outside the organism, but both need to modify the seawater chemistry for

623   calcification to take place (Roleda et al. 2012). It is thought that HCO$_3^-$ is the choice of substrate for

624   biomineralisation, which can be taken directly from seawater or metabolised from CO_2 (Roleda et al.

625   2012). The mechanisms revolve around producing an abundance of ions and the right conditions to

626   favour the precipitation of $CaCO_3$ from available Ca^{2+} and CO_3^{2-} (Roleda et al. 2012). An understanding

627   of biomineralisation mechanisms under forecasted OA conditions will require the use of a wide range

628   of techniques (Figure 5) but also working at different levels, from genes to organisms and ecosystems.

629   This can be achieved by taking advantage of established techniques from other disciplines. For example,

630   methods to culture larval sea urchin primary mesenchyme cells facilitates the study of the calcification

631   process *in vitro* (Basse et al. 2015). Identifying and evaluating the roles of organic molecules in shells

632   is a major topic in biomineralisation as the mechanical properties of shells are highly influenced by

633   their 1% content of organic components. In the context of OA impacts on marine calcifiers, the response

634   of organic molecules provides an insight into cellular mechanisms for the ability to reproduce and

635   develop and can be applied to all marine organisms irrespective of size (Figure 1, schematic of question

636   vs scale). Mechanisms of biomineralisation are largely unresolved and vary from species to species.
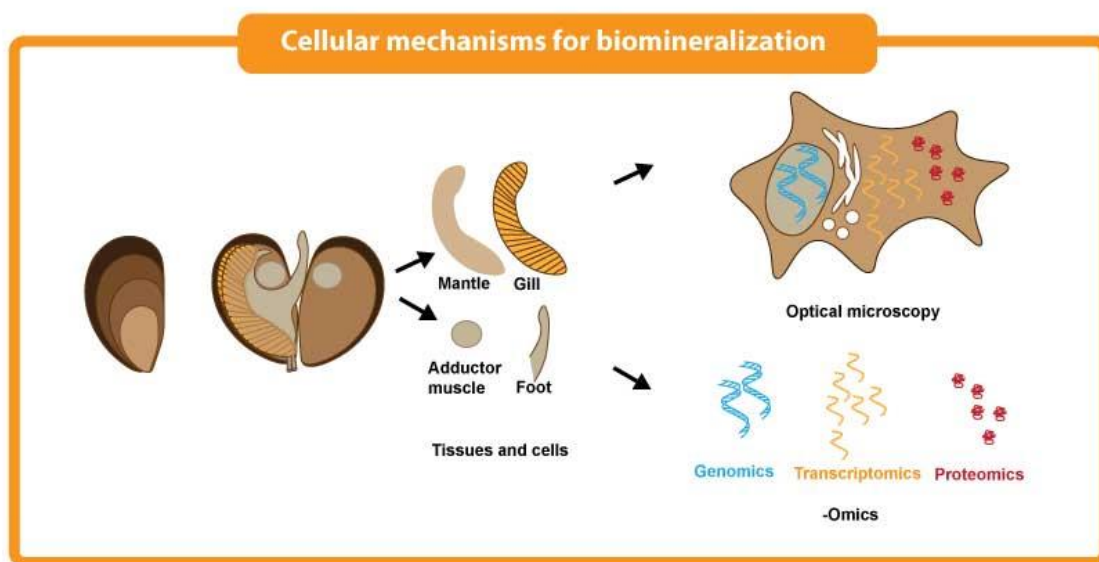
637

638   **Figure 5. Schematic representation of techniques to examine the cellular mechanism of**

639   **biomineralisation. Techniques with OMICS, optical microscopy are established techniques that**

640   **could be applied on various tissues and cells to determine the impact of OA on molecular**

641   **biomineralisation.**

29

642

643 *SDS-PAGE and MS*

644 Shell protein extraction is achieved by recovering the protein from decalcified shell. Sodium dodecyl

645 sulfate-polyacrylamide gel electrophoresis (SDS-PAGE), or 2D gel electrophoresis enables a

646 comparison of protein profiles. In addition, mass spectrometry (MS) also enables the identification of

647 proteins from available databases. As marine organisms studied in OA research are usually not 'model-

648 organisms', protein identification is challenging. Protein purification, protein sequencing, and protein

649 digestion, may be required in the identification process (Marxen et al. 2003, Suzuki et al. 2004). When

650 a large protein (more than 30 kDa) needs to be identified, cloning methods can be used to recover the

651 nucleotide sequence for deduction of the protein sequence (Miyamoto et al. 1996, Samata et al. 1999,

652 Suzuki et al. 2009, Suzuki et al. 2011). Many genome and transcriptome databases of calcifying

653 invertebrates generated by next generation sequencing are also available as open resources (Takeuchi

654 et al. 2012, Zhang et al. 2012).

655 MS is also a promising technique to understand shell proteins. The MS/MS spectra of peptides allow

656 determination of amino acid sequence without the need for a protein sequencer and has become a low

657 cost and high throughput technique. The combination of MS/MS and databases from next generation

658 sequencing is dramatically increasing the efficiency of protein identification (Joubert et al. 2010,

659 Marie et al. 2010, Marie et al. 2011). The potential disadvantage of generating big data from the high

660 throughput process is covered in more detail in the next Section. These techniques have been applied

661 to show the proteome responses of invertebrates grown in OA conditions. For example, the shell

662 matrix proteins of the larval pacific oyster (*Magallana gigas*) were observed to decrease under OA

663 (Harney et al. 2016).

664 SDS-PAGE and MS offer advantages of low cost and in the case of MS high throughput protein

665 identification to understand why physiological responses may be influenced by ocean acidification.

666 The disadvantages of these techniques include time-consuming sample preparation to extract and

667 purify proteins for analysis and production of big data which can be difficult to interpret.

Insoluble organic component analyses using XRD, IR and pyrolysis NMR, and dyes

669   Insoluble organic components in the shell, such as chitin, are an essential polysaccharide that connects

670   organic matrices and the initial deposition of the mineral (Nakayama et al. 2013); it serves as a scaffold

671   for organic materials during the deposition of minerals. For example, the molluscan periostracum is

672   made of chitin and it serves as a waterproof layer of a calcification compartment. Chitin is commonly

673   found in the forms of α and β-chitin. Crustaceans use α-chitin in their exoskeletons and molluscs use β-

674   chitin in their shells, as such, chitin is an essential additive to greatly improve the mechanical properties

675   of biomaterials. Due to the insoluble and organic nature of chitin, the impact of OA on chitin content is

676   currently unknown. There are many techniques to identify chitin, including X-ray diffraction (Weiner

677   and Traub 1980, Levi-Kalisman et al. 2001, Falini et al. 2003), infra-red (IR) spectroscopy in the finger

678   printing region (700-1800 cm^{-1}) (Pearson et al. 1960), and nuclear magnetic resonance (NMR) or MS

679   detection of the glucosamine hydrochloride after hydrolysis (Nakayama et al. 2013). The analysis of

680   pyrolysis (thermal decomposition of materials in a vacuum) GC-MS is able to identify characteristic

681   chitin decomposition markers (Furuhashi et al. 2009). However, many other contaminants (such as

682   proteins) produce a complex of unknown peaks that make the identification of chitin in biominerals

683   difficult and, in the case of insufficient crystallinity, a clear diffraction pattern may be hard to obtain.

684   Recently, a colorimetric assay of chitin has been developed to quantify chitin (Katano et al. 2016). The

685   workers found that upon complete hydrolysis of chitin in strong acid (5M HCl), characterization of

686   depolymerized glucosamine is possible using colorimetry at the absorbance maximum at 750 nm. The

687   method requires small amount of sample (10 mg), it is low cost, simple and quantitative. However, the

688   detection is robust and cannot distinguish polymorphs and spatial distribution of chitin.

689   Chitin can be visualised microscopically by calcofluor white which binds strongly to cellulose and

690   chitin, and wheat-germ agglutinin (WGA) which binds to N-acetyl-D-glucosamine and sialic acid

691   (Suzuki et al. 2007). Due to the non-specific nature of calcofluor-white and WGA, more specific

692   detection is accomplished by using chitin-binding domain fused with green fluorescent protein (CBD-

693   GFP) as shown in the larval shell of *Mytilus galloprovincialis* (Weiss and Schönitzer 2006) and the

694   prismatic layer of *Atrina rigida* (Nudelman et al. 2007). Quantifying the expression of the chitin

695   synthase gene is an alternative approach to measure chitin production (Cummings et al. 2011).

696   While the role of chitin may be essential in providing a waterproof cover and biomineralisation

697   framework to the shell formation process, the plasticity of chitin synthesis under OA environmental

698   stress has not yet been investigated. Chitin has many important biological roles in a diverse taxonomic

699   group of animal models (Lee et al. 2011), therefore, the detection of chitin could provide valuable

700   information on both the structural and functional responses to OA. The disadvantages of XRD, IR, and

701   pyrolysis NMR or GC-MS techniques for chitin analysis such as the low abundance of organic materials

702   in calcareous structures and therefore time-consuming sample preparation may limit the application of

703   this approach to future OA studies. On the other hand, visualizing chitin with dyes such as calcofluor

704   white and WGA are prone to non-specific reactivity to other molecules than chitin. The more specific

705   CBD-GFP labeling requires bioengineering protocol to express and purify the chitin probe.

706   *OMICS*

707   Omics studies are generating "big data". However, these data cannot be simply used as proxies of fitness

708   (Feder and Walser 2005). As a consequence, little information can be extracted from purely exploratory

709   studies (e.g. comparisons between two OA scenarios). A more powerful approach involves the analysis

710   of the data to test a hypothesis based on physiological or ecological experiments. For example, De Wit

711   et al. (2016) filtered a large-scale transcriptomic database to select genes following the same pattern

712   identified at the physiological level in copepods exposed to OA (Thor and Dupont 2015, De Wit et al.

713   2016). The future use of omics to investigate the effects of OA on biomineralisation is promising,

714   especially using the integration of omics technique with other physiological endpoints.

715   The three main omics approaches to consider are transcriptomics, proteomics and metabolomics.

716   Transcriptomics is a study of mRNA and actively expressed genes, while proteomics investigates the

717   total protein profile, and metabolomics capture the biochemical status of an organism.

718   Transcriptomic changes can provide insights into genetic pathways involved in calcification by

719   comparison of gene expression, for example at different stages of calcification, or under different

720 environmental conditions. That is, when applied in a time series, changes in transcriptomes of

721 developing larvae provide useful information relevant to the onset of biomineralisation (Zhang et al.

722 2012). De Wit et al. (2018) used OA as a tool to delay calcification in early stage of oyster development

723 and using a time series were able to identify genes involved in larval shell calcification (De Wit et al.

724 2018). Under OA, transcriptomic studies are used to assess the physiological capacity of organisms by

725 studying not just the biomineralisation molecular pathways but also the other related pathways giving

726 a complete picture in understanding the consequences of living in a high CO_2 oceans (Todgham and

727 Hofmann 2009).

728 Proteomics investigates the total protein profile. Since proteins are the active functional units of an

729 expressed gene, these data are closer to the organism at the functional level and phenotype. Proteomes

730 can be altered by OA, as shown by different calcification protein expression in oysters (Dineshram et

731 al. 2015). The organic matrix proteins that are associated to shell deposition have been profiled in corals

732 (Drake et al. 2013), oysters (Suzuki and Nagasawa 2013), and blue mussels (Suzuki et al. 2011),

733 although this information has not been profiled in the OA context.

734 In common with the transcriptome, some precautions should be taken during the interpretation of a

735 proteome. The quantity of a protein commonly cannot be directly linked to the fitness of an organism

736 as regulatory post-translational modifications play a key role (Mann and Jensen 2003). This is an

737 essential consideration for the study of shell proteins which are often heavily glycosylated,

738 phosphorylated or tyrosine sulfated as required for calcium binding (Zhang and Zhang 2006).

739 A major disadvantage of applying OMICS to the study of biomineralisation is the low abundance of

740 about 5% organic content in calcareous structures (Zhang and Zhang 2006). In order to isolate sufficient

741 protein or polysaccharide for analysis, a large amount of shell must be used. In addition, the extraction

742 and purification of the organic content is greatly influenced by decalcification, and the shell can often

743 contain organic impurities (Watabe 1965). Researchers should be aware of technical limitations using

744 different characterisation techniques, for example 2D gels have a lower sensitivity than iTRAQ analysis

745 (Wiese et al. 2007). In addition, the interpretation of OMICS data is highly dependent on genomic

746 information, therefore, it remains as a challenging method for non-model organisms.

33

747 *Cellular pH imaging*

748 When live imaging is conducted, inverted microscopy enables living marine organisms to be fully

749 submersed in seawater during observation (Venn et al. 2011, Stumpp et al. 2012, Tambutté et al. 2015,

750 Chan et al. 2017). In some imaging methods, synthetic ratiometric images are generated by sequential

751 images of the same region of interest. Mobile organisms can be immobilized (e.g. 2-4% agarose

752 seawater or using micropipettes) to enable image acquisition of the region of interest. For longer periods

753 of observation, a perfusion chamber is necessary to remove metabolic waste and allow exchange of

754 aerated experimental seawater with enriched CO_2.

755 Fluorescent microscopy has been applied to visualise the calcification compartment during

756 mineralisation at a low seawater pH using markers including calcein, alizarin and calcofuor white for

757 *in situ* analysis of calcification and tracking of calcification as shown for coralline algae (Lewis and

758 Diaz-Pulido 2017). Newly deposited minerals can be quantified from their fluorescent appearance at

759 their respective excitation ($Ex\lambda$) and emission wavelengths ($Em\lambda$), e.g. alizarin: $Ex\lambda$ = 530-560 nm,

760 $Em\lambda$ = 580 nm; calcein: $Ex\lambda$ = 494 nm, $Em\lambda$ = 517 nm; calcofluor white: $Ex\lambda$ = 365 nm, $Em\lambda$ = 435

761 nm. Calcein is a preferable marker because of its high efficiency, non-invasiveness (Lewis and Diaz-

762 Pulido 2017) and it is relatively low in cost. In addition, the fluorescent region can be isolated and

763 characterised using the techniques described for measuring growth and development in the earlier

764 sections .

765 The heterogenous distribution of carbon sources, e.g. CO_3^{2-} ions at the calcification site, can be

766 monitored by measuring intracellular pH (de Nooijer et al. 2008, Venn et al. 2011, Venn et al. 2013,

767 Tambutté et al. 2015). Similar to the carbonate dynamics in the ocean, a shift in pH influences the DIC

768 abundance in the biomineralisation compartment, in terms of CO_3^{2-} and HCO_3^-. As shown in

769 foraminifera, pH of the site of calcification increases during calcification, while the surrounding

770 ambient pH decreases probably through active proton pumping (Toyofuku et al. 2017). A higher pH

771 value facilitates the conversion of CO_2 and HCO_3^- to CO_3^{2-} (Toyofuku et al. 2017), and both the CO_3^{2-}

772 concentration and calcium carbonate saturation state can then be calculated (Venn et al. 2011, Venn et

773 al. 2013, Tambutté et al. 2015). Furthermore, it is possible to estimate the amount of emitted proton by

774   image processing of pH sensitive ratiometric microsopy. Ratiometric fluorescent dyes enable the

775   monitoring of intracellular and extracellular pH (Chan et al. 2015a, Comeau et al. 2017b, Toyofuku et

776   al. 2017). Several pH sensitive dyes are available depending on the tested pH range. When the cell

777   permeable dye SNARF-1 acetoxymethyl ester is excited at a wavelength of 543 nm, the ratio of

778   fluorescence captured at emission wavelengths of 585 ± 10 nm and 640 ± 10 nm shows a linear

779   relationship to intracellular pH (Venn et al. 2013). Similarly, cell impermeable SNARF-1 can be used

780   to measure pH in the calcifying fluid in corals; 2'-7'-bis(carboxyethyl)-5(6)-carboxyfluorescein

781   (BCECF) for intracellular pH of echinoderm larvae (Stumpp et al. 2012) and pyranine for foraminifera

782   (Toyofuku et al. 2017). This technique has been applied to OA to investigate how growth and

783   calcification rates are impacted by increasing pCO$_2$ (Stumpp et al. 2012), where extracellular pH was

784   actively compensated.

785   More recently, measurement of intracellular pH employs the use of microelectrodes between 10 and 15

786   µm tip diameter for direct in-tissue measurement (Cai et al. 2016), using pH polymeric membrane

787   microelectrodes (Zhao and Cai 1999), and CO$_3^{2-}$ electrodes (Cai et al. 2016). Using this approach, pH

788   and CO$_3^{2-}$ were observed to sharply increase in the calcifying fluid of various coral species, confirming

789   the presence of H$^+$ pump (Cai et al. 2016). In addition to intracellular pH determination, microelectrodes

790   can be designed to monitor dissolved oxygen and calcium concentration to enable analysis of a wider

791   range of parameters (Glas et al. 2012a, Glas et al. 2012b). The cellular pH imaging techniques have an

792   advantage of high spatial resolution for direct in-tissue measurement, however, the disadvantages

793   include time consuming sample preparation. This includes the challenge that organism immobilization

794   strategies varies and the protocol requires optimization to ensure the organism is capable of generating

795   biominerals. Ratiometric pH probe also requires calibration before the ratios can be converted to pH

796   values.

797   *Physiological inhibitors and stimulators*

798   The use of physiological inhibitors or stimulators is a useful approach to investigate the biochemical

799   pathways and pumps involved with biomineralisation (Basse et al. 2015). How biological pathways

800   may be influenced by specific inhibitors can explain the mechanism of shell formation under OA

801   conditions. For example, treatment with adenylyl cyclase inhibitors alleviate the negative effects of OA

802   in Pacific oysters, suggesting the potential mechanism change under OA (Wang et al. 2017). This result

803   confirmed the role of adenosine triphosphate (ATP) generation is essential to support shell production

804   (Pan et al. 2015). Not requiring complete genetic information is greatest advantage of using inhibitors

805   and stimulators to evaluate the mechanisms of biomineralization in a reductionist approach (Toyofuku

806   et al. 2017). However, the choice of inhibitors may be non-specific to a single pathway and its action

807   requies verification by a known physiological end-point.

808   **Combining techniques**

809   The described techniques can be employed individually to answer specific scientific questions to

810   determine the impact of OA on marine biomineralisation. However, it is important to consider

811   combining techniques to address complex scientific questions.

812   *Combining x-ray microscopy techniques*

813   Due to the development of optimum sample preparation for the analysis of a flat surface (Perez-Huerta

814   and Cusack 2009), the output of XPEEM with XAS (Fitzer et al. 2016) and SEM-EBSD (Hahn et al.

815   2012, Wolfe et al. 2013, Fitzer et al. 2014a, Fitzer et al. 2014b) can be readily compared. This has

816   allowed the influence of OA on both the biomineral structure and composition to be determined for

817   corals (Rodolfo-Metalpa et al. 2011), sea urchins (Bray et al. 2014), and mussels (Melzner et al. 2011).

818   Likewise, the simple mapping of calcite and aragonite is applicable across a wide variety of species

819   including mussels and limpets (Hahn et al. 2012, Langer et al. 2014, Fitzer et al. 2015a). In contrast,

820   comparison of mineral composition between high-resolution microscopy with spectral techniques such

821   as XRD, FT-IR, and XPEEM with XAS is more complex. The use of SEM imaging, and calcite and

822   aragonite thickness by EBSD, or species-specific visual inspection using compound microscopy (Fitzer

823   et al. 2014b), have their merits to examine larger areas of shell erosion. However, to examine the

824   intricate details of biomineralisation and potential changes under OA conditions these methods should

825   be used in conjunction with XRD, FT-IR, XPEEM with XAS, and SEM-EBSD.

826   *Multi-omics data integration*

827 Several -omics approaches can be integrated, i.e. multi-omics (Huang et al. 2017). For example, the

828 mantle transcriptome and shell proteomes were integrated to study the shell formation of the pearl oyster

829 (Joubert et al. 2010, Berland et al. 2011), enabling proteomics data to be analysed without a complete

830 genome. Similarly, proteomics and metabolomics were studied together in oysters (Wei et al. 2015). A

831 more complex multi-omics study examined the genome, transcriptome and proteome in the Pacific

832 oyster (Zhang et al. 2012). Such a multi-omics approach also provided insights on the phosphate

833 biomineralisation in brachiopods (Luo et al. 2015). This is a promising approach in the context of OA

834 to understand the fitness or survival of organisms.

835 **Conclusions: What now for OA research on biomineralisation?**

836 A range of tools are shown in this article to help researchers to determine the impact of OA on

837 biomineralisation mechanisms at physiological and molecular levels, and thus on shell or skeleton

838 structural mechanics. The purpose of this review is to discuss commonly available biomineralisation

839 tools for understanding this one physiological response to ocean acidification. However, organisms

840 have a complex physiological profiles, and it is important to note that biomineralisation is not an isolated

841 process, and not is it the only physiological process that needs to be considered in this context. Given

842 the nature of biomineralisation mechanisms and their complex responses to OA, a variety of

843 physiological, materials science, and crystallography tools are needed to thoroughly understand the

844 biomineralisation process and its vulnerability to OA. This review outlines techniques that can be used

845 to characterise, quantify and monitor the process of biomineralisation in a variety of calcifying marine

846 organisms, especially when they are cultured under OA experimental conditions. It also highlights basic

847 principles and the advantages and disadvantages of established, emerging and future techniques for OA

848 researchers. The key to developing a strategy aimed at better understanding the potential consequences

849 of OA is to define clear questions and hypotheses for testing. This would naturally lead to constrains

850 (e.g. tested species, quantity of material available, size) that, when combined with practicalities (e.g.

851 budget, equipment), will lead to selection of the appropriate experimental approach.

852 Recently, more attention has been paid to the underlying biological and physiological mechanisms of

853 biomineralisation. For example, tissues and external organic layers can protect the shell from corrosion

37

854 in under-saturated waters (Rodolfo-Metalpa et al. 2011). To address the underlying mechanisms

855 affected by the impacts by OA, various methods need to be combined. For instance, determination of

856 amorphous calcium carbonate is important to characterise mineral choice and relate phase transitions at

857 the earliest stage of biomineral formation. Mechanisms of cellular involvement and specific

858 biomolecules for biomineralisation can be examined using fluorescent microscopy and omics. The

859 interactions of proteins in the extrapallial fluid and shell interface can be understood by applying

860 techniques in isotope labelling and microscopy. It is also crucial to consider the fitness consequences

861 of observed changes. For example, in a prey species, shell strength should be considered in relation to

862 predator behaviour. The combination of established, emerging and future techniques will enable a

863 holistic approach and better understanding of the potential impact of OA on biomineralisation by marine

864 species and consequences for marine calcifiers and associated ecosystems.

870 **References**

871 Addadi, L., Raz, S., and Weiner, S. 2003. Taking advantage of disorder: Amorphous calcium

872   carbonate and its roles in biomineralization. *Advanced Materials* **15**:959-970.

873 Alfredsson, V. 2005. Cryo-TEM studies of DNA and DNA–lipid structures. *Current Opinion in*

874   *Colloid & Interface Science* **10**:269-273.

875 Allen, K.A., Hönisch, B., Eggins, S.M., and Rosenthal, Y. 2012. Environmental controls on B/Ca in

876   calcite tests of the tropical planktic foraminifer species *Globigerinoides ruber* and

877   *Globigerinoides sacculifer*. *Earth and Planetary Science Letters* **351–352**:270-280.

878 Allison, N., Cohen, I., Finch, A.A., Erez, J., and Tudhope, A.W. 2014. Corals concentrate dissolved

879   inorganic carbon to facilitate calcification. *Nature Communications* **5**:5741.

880   Anstis, G., Chantikul, P., Lawn, B.R., and Marshall, D. 1981. A critical evaluation of indentation

881   techniques for measuring fracture toughness: I, direct crack measurements. *Journal of the*

882   *American Ceramic Society* **64**:533-538.

883   Asnaghi, V., Chiantore, M., Mangialajo, L., Gazeau, F., Francour, P., Alliouane, S., and Gattuso, J.P.

884   2013. Cascading effects of ocean acidification in a rocky subtidal community. *PLOS ONE*

885   **8**:e61978

886   Basse, W.C., Gutowska, M.A., Findeisen, U., Stumpp, M., Dupont, S., Jackson, D.J., Himmerkus, N.,

887   Melzner, F., and Bleich, M. 2015. A sea urchin Na+K+2Cl− cotransporter is involved in the

888   maintenance of calcification-relevant cytoplasmic cords in *Strongylocentrotus droebachiensis*

889   larvae. *Comparative Biochemistry and Physiology Part A: Molecular & Integrative*

890   *Physiology* **187**:184-192.

891   Becker, J.S., Breuer, U., Hsieh, H.F., Osterholt, T., Kumtabtim, U., Wu, B., Matusch, A., Caruso,

892   J.A., and Qin, Z. 2010. Bioimaging of metals and biomolecules in mouse heart by laser

893   ablation inductively coupled plasma mass spectrometry and secondary ion mass spectrometry.

894   *Analytical Chemistry* **82**:9528-9533.

895   Beniash, E., Ivanina, A., Lieb, N.S., Kurochkin, I., and Sokolova, I.M. 2010. Elevated level of carbon

896   dioxide affects metabolism and shell formation in oysters *Crassostrea virginica*. *Marine*

897   *Ecology Progress Series* **419**:95-108.

898   Berland, S., Marie, A., Duplat, D., Milet, C., Sire, J.Y., and Bédouet, L. 2011. Coupling proteomics

899   and transcriptomics for the identification of novel and variant forms of mollusk shell proteins:

900   a study with *P. margaritifera*. *Chembiochem* **12**:950-961.

901   Bernhard, J.M., Blanks, J.K., Hintz, C.J., and Chandler, G.T. 2004. Use of the fluorescent calcite

902   marker calcein to label foraminiferal tests. *Journal of Foraminiferal Research* **34**:96-101.

903   Bradassi, F., Cumani, F., Bressan, G., and Dupont, S. 2013. Early reproductive stages in the crustose

904   coralline alga Phymatolithon lenormandii are strongly affected by mild ocean acidification.

905   *Marine Biology* **160**:2261-2269.

906   Bray, L., Pancucci-Papadopoulou, M.A., and Hall-Spencer, J.M. 2014. Sea urchin response to rising

907   pCO_2 shows ocean acidification may fundamentally alter the chemistry of marine skeletons.

908   *Mediterranean Marine Science* **15**(3):510-519. doi: http://dx.doi.org/10.12681/mms.579

909   Butt, H.-J., Cappella, B., and Kappl, M. 2005. Force measurements with the atomic force microscope:

910   Technique, interpretation and applications. *Surface Science Reports* **59**:1-152.

911   Butt, H.-J., Jaschke, M., and Ducker, W. 1995. Measuring surface forces in aqueous electrolyte

912   solution with the atomic force microscope. *Bioelectrochemistry and Bioenergetics* **38**:191-

913   201.

914   Byrne, M., Lamare, M., Winter, D., Dworjanyn, S.A., and Uthicke, S. 2013. The stunting effect of a

915   high CO_2 ocean on calcification and development in sea urchin larvae, a synthesis from the

916   tropics to the poles. *Philosophical transactions of the Royal Society of London. Series B,*

917   *Biological sciences* **368**:20120439. doi: 10.1098

918   Byrne, M., Smith, A.M., West, S., Collard, M., Dubois, P., Graba-landry, A., and Dworjanyn, S.A.

919   2014. Warming influences Mg^{2+} content, while warming and acidification influence

920   calcification and test strength of a sea urchin. *Environmental science & technology* **48**:12620-

921   12627.

922   Cai, W.-J., Ma, Y., Hopkinson, B.M., Grottoli, A.G., Warner, M.E., Ding, Q., Hu, X., Yuan, X.,

923   Schoepf, V., Xu, H., Han, C., Melman, T.F., Hoadley, K.D., Pettay, D.T., Matsui, Y.,

924   Baumann, J.H., Levas, S., Ying, Y., and Wang, Y. 2016. Microelectrode characterization of

925   coral daytime interior pH and carbonate chemistry. *Nature Communications* **7**:11144. doi:

926   10.1038/ncomms11144

927   Carricart-Ganivet, J.P., and Barnes, D.J. 2007. Densitometry from digitized images of X-radiographs:

928   Methodology for measurement of coral skeletal density. *Journal of Experimental Marine*

929   *Biology and Ecology* **344**:67-72.

930   Chan, V.B.S., Toyofuku. T., Wetzel, G., Saraf, L., Thiyagarajan, V., and Mount, A. S. 2017.

931   Characterization of calcification events using live optical and electron microscopy techniques

932   in a marine tubeworm. *Journal of Visualized Experiments*:e55164-e55164.

933   Chan, V.B.S., Li., C, Lane, A.C., Wang, Y., Lu, X., Shih, K., Zhang, T., and Thiyagarajan, V. 2012.

934   CO_2-driven ocean acidification alters and weakens integrity of the calcareous tubes produced

935   by the serpulid tubeworm, *Hydroides elegans*. *PLOS ONE* **7**:e42718

936   Chan, V.B.S., Toyofuku, T., Wetzel, G., Saraf, L., Thiyagarajan, V., and Mount, A.S. 2015a. Direct

937   deposition of crystalline aragonite in the controlled biomineralization of the calcareous

938   tubeworm. *Frontiers in Marine Science* **2**(97):1-10. doi: 10.3389/fmars.2015.00097

939   Chan, V.B.S., Vinn, O., Li, C., Lu, X., Kudryavtsev, A.B., Schopf, J.W., Shih, K., Zhang, T., and

940   Thiyagarajan, V. 2015b. Evidence of compositional and ultrastructural shifts during the

941   development of calcareous tubes in the biofouling tubeworm, *Hydroides elegans*. *Journal of*

942   *structural biology* **189**:230-237.

943   Chatzinikolaou, E., Grigoriou, P., Keklikoglou, K., Faulwetter, S., and Papageorgiou, N. 2017. The

944   combined effects of reduced pH and elevated temperature on the shell density of two

945   gastropod species measured using micro-CT imaging. *ICES Journal of Marine Science:*

946   *Journal du Conseil* **74**:1135-1149.

947   Collard, M., Rastrick, S.P.S., Calosi, P., Demolder, Y., Dille, J., Findlay, H.S., Hall-Spencer, J.M.,

948   Milazzo, M., Moulin, L., Widdicombe, S., Dehairs, F., and Dubois, P. 2016. The impact of

949   ocean acidification and warming on the skeletal mechanical properties of the sea urchin

950   *Paracentrotus lividus* from laboratory and field observations. *ICES Journal of Marine*

951   *Science* **73**:727-738.

952   Comeau, S., Cornwall, C.E., and McCulloch, M.T. 2017a. Decoupling between the response of coral

953   calcifying fluid pH and calcification to ocean acidification. *Scientific Reports* **7**:7573.

954   doi:10.1038/s41598-017-08003-z

955   Comeau, S., Tambutte, E., Carpenter, R.C., Edmunds, P.J., Evensen, N.R., Allemand, D., Ferrier-

956   Pages, C., Tambutte, S., and Venn, A.A. 2017b. Coral calcifying fluid pH is modulated by

957   seawater carbonate chemistry not solely seawater pH. *Proceedings of the Royal Society B-*

958   *Biological Sciences* **284**: 20161669. doi: 10.1098/rspb.2016.1669

959 Cooper, T.F., De'Ath, G., Fabricius, K.E., and Lough, J.M. 2008. Declining coral calcification in
960   massive Porites in two nearshore regions of the northern Great Barrier Reef. *Global Change*
961   *Biology* **14**:529-538.

962 Cummings, V., Hewitt, J., Van Rooyen, A., Currie, K., Beard, S., Thrush, S., Norkko, J., Barr, N.,
963   Heath, P., Halliday, N.J., Sedcole, R., Gomez, A., McGraw, C., and Metcalf, V. 2011. Ocean
964   acidification at high latitudes: potential effects on functioning of the Antarctic bivalve
965   *Laternula elliptica. PLOS ONE* **6**:e16069

966 Cyronak, T., Schulz, K.G., and Jokiel, P.L. 2016. The Omega myth: what really drives lower
967   calcification rates in an acidifying ocean. *ICES Journal of Marine Science* **73**:558-562.

968 Dalbeck, P., Cusack, M., Dobson, P.S., Allison, N., Fallick, A.E., and Tudhope, A.W. 2011.
969   Identification and composition of secondary meniscus calcite in fossil coral and the effect on
970   predicted sea surface temperature. *Chemical Geology* **280**:314-322.

971 Davies, P.S. 1989. Short-term growth measurements of corals using an accurate buoyant weighing
972   technique. *Marine Biology* **101**:389-395.

973 de Nooijer, L.J., Toyofuku, T., Oguri, K., Nomaki, H., and Kitazato, H. 2008. Intracellular pH
974   distribution in foraminifera determined by the fluorescent probe HPTS. *Limnology and*
975   *Oceanography: Methods* **6**:610-618.

976 De Wit, P., Dupont, S., and Thor, P. 2016. Selection on oxidative phosphorylation and ribosomal
977   structure as a multigenerational response to ocean acidification in the common copepod
978   Pseudocalanus acuspes. *Evolutionary Applications* **9**:1112-1123.

979 De Wit, P., Durland, E., Ventura, A., and Langdon, C.J. 2018. Gene expression correlated with delay
980   in shell formation in larval Pacific oysters (*Crassostrea gigas*) exposed to experimental ocean
981   acidification provides insights into shell formation mechanisms. *Bmc Genomics* **19**:160.

982 deVries, M.S., Webb, S.J., Tu, J., Cory, E., Morgan, V., Sah, R.L., Deheyn, D.D., and Taylor, J.R.A.
983   2016. Stress physiology and weapon integrity of intertidal mantis shrimp under future ocean
984   conditions. *Scientific Reports* **6**:38637.

985   Dickinson, G.H., Ivanina, A.V., Matoo, O.B., Portner, H.O., Lannig, G., Bock, C., Beniash, E., and
986   Sokolova, I.M. 2012a. Interactive effects of salinity and elevated CO_2 levels on juvenile
987   eastern oysters, *Crassostrea virginica*. *The Journal of Experimental Biology* **215**:29-43.

988   Dickinson, G.H., Ivanina, A.V., Matoo, O.B., Pörtner, H.O., Lannig, G., Bocl, C., Beniash, E., and
989   Sokolova, I.M. 2012b. Interactive effects of salinity and elevated CO_2 levels on juvenile
990   eastern oysters, *Crassostrea virginica*. *Journal of Experimental Biology* **215**:29-43.

991   Dineshram, R., Sharma, R., Chandramouli, K., Yalamanchili, H.K., Chu, I., and Thiyagarajan, V.
992   2015. Comparative and quantitative proteomics reveal the adaptive strategies of oyster larvae
993   to ocean acidification. *Proteomics* **15**:4120-4134.

994   Doney, S.C., Fabry, V.J., Feely, R.A., and Kleypas, J.A. 2009. Ocean acidification: the other CO_2
995   problem. *Annual Review of Marine Science* **1**:169-192.

996   Drake, J.L., Mass, T., Haramaty, L., Zelzion, E., Bhattacharya, D., and Falkowski, P.G. 2013.
997   Proteomic analysis of skeletal organic matrix from the stony coral *Stylophora pistillata*.
998   *Proceedings of the National Academy of Sciences* **110**:3788-3793.

999   Dwyer, G.S., Cronin, T.M. and Baker, P.A. 2013. Trace elements in marine ostracodes. In
1000   J.A.Holmes & A.R.Chivas (eds) *The Ostracoda: Applications in Quaternary Research.*
1001   *Geophys. Monogr. Series.*, AGU, Washington. Pages 205-225.

1002   Eichner, M.J., Klawonn, I., Wilson, S.T., Littmann, Whitehouse, S.M.J., Church, M.J., Kuypers,
1003   M.M.M., Karl, D.M., and Ploug, H. 2017. Chemical microenvironments and single-cell
1004   carbon and nitrogen uptake in field-collected colonies of Trichodesmium under different
1005   *p*CO_2. *The Isme Journal* **11**:1305.

1006   Eisenstein, N.M., Cox, S.C., Williams, R.L., Stapley, S.A., and Grover, L.M. 2016. Bedside,
1007   benchtop, and bioengineering: physicochemical imaging techniques in biomineralization.
1008   *Advanced healthcare materials* **5**:507-528.

1009   Elderfield, H., Bertram, C.J., and Erez, J. 1996. A biomineralization model for the incorporation of
1010   trace elements into foraminiferal calcium carbonate. *Earth and Planetary Science Letters*
1011   **142**:409-423.

1012   Erez, J. 1978. Vital effect on stable-isotope composition seen in foraminifera and coral skeletons.

1013   *Nature* **273**:199.

1014   Falini, G., Weiner, S., and Addadi, L. 2003. Chitin-silk fibroin interactions: relevance to calcium

1015   carbonate formation in invertebrates. *Calcified tissue international* **72**:548-554.

1016   Fang, J.K., Schoenberg, C.H., Kline, D.I., Hoegh-Guldberg, O., and Dove, S. 2013. Methods to

1017   quantify components of the excavating sponge *Cliona orientalis* Thiele, 1900. *Marine*

1018   *Ecology* **34**:193-206.

1019   Fantazzini, P., Mengoli, S., Pasquini, L., Bortolotti, V., Brizi, L., Mariani, M., Di Giosia, M.,

1020   Fermani, S., Capaccioni, B., Caroselli, E., Prada, F., Zaccanti, F., Levy, O., Dubinsky, Z,

1021   Kaandorp, J.A., Konglerd, P., Hammel, J.U., Dauphin, Y., Cuif, J.-P., Weaver, J.C.,

1022   Fabricius, K.E., Wagermaier, W., Fratzl, P., Falini, G., and Goffredo, S. 2015. Gains and

1023   losses of coral skeletal porosity changes with ocean acidification acclimation. *Nature*

1024   *Communications* **6**:7785. doi: 10.1038/ncomms8785

1025   Feder, M.E., and Walser, J.C. 2005. The biological limitations of transcriptomics in elucidating stress

1026   and stress responses. *Journal of evolutionary biology* **18**:901-910.

1027   Fietzke, J., Heinemann, A., Taubner, I., Böhm, F., Erez, J., and Eisenhauer, A. 2010. Boron isotope

1028   ratio determination in carbonates via LA-MC-ICP-MS using soda-lime glass standards as

1029   reference material. *Journal of Analytical Atomic Spectrometry* **25**:1953-1957.

1030   Fitzer, S. Chung, C.P., Maccherozzi, F., Dhesi, S.S., Kamenos, N.A., Phoenix, V.R., and Cusack,

1031   M.2016. Biomineral shell formation under ocean acidification: a shift from order to chaos.

1032   *Scientific Reports* **6**:21076. doi: 10.1038/srep21076

1033   Fitzer, S.C., Cusack, M., Phoenix, V.R., and Kamenos, N.A. 2014a. Ocean acidification reduces the

1034   crystallographic control in juvenile mussel shells. *Journal of structural biology* **188**:39-45.

1035   Fitzer, S.C., Phoenix, V.R., Cusack, M., and Kamenos, N.A. 2014b. Ocean acidification impacts

1036   mussel control on biomineralisation. *Scientific Reports* **4**:6218. doi: 10.1038/srep06218

1037   Fitzer, S.C., Vittert, L., Bowman, A., Kamenos, N.A., Phoenix, V.R., and Cusack, M. 2015a. Ocean

1038   acidification and temperature increase impact mussel shell shape and thickness: problematic

1039   for protection? *Ecology and Evolution* **5**:4875-4884.

1040 Fitzer, S.C., Zhu, W., Tanner, K.E., Kamenos, N.A., Phoenix, V.R., and Cusack, M. 2015b. Ocean

1041   acidification alters the material properties of *Mytilus edulis* shells. *Journal of the Royal*

1042   *Society Interface* **12**:20141227.

1043 Freeman, A.S., and Byers J.E. 2006. Divergent induced responses to an invasive predator in marine

1044   mussel populations. *Science* **313**:831-833.

1045 Frieder, C.A., Applebaum, S.L., Pan, T.C.F., Hedgecock, D, and Manahan, D.T. 2016. Metabolic cost

1046   of calcification in bivalve larvae under experimental ocean acidification. *ICES Journal of*

1047   *Marine Science*. **74**(4):941-954. doi:https://doi.org/10.1093/icesjms/fsw213

1048 Fu, J.M., He, C., Xia, B., Li, Y., Feng, Q., Yin, Q.F., Shi, X.H., Feng, X., Wang, H.T., and Yao, H.M.

1049   2016. c-axis preferential orientation of hydroxyapatite accounts for the high wear resistance

1050   of the teeth of black carp (*Mylopharyngodon piceus*). *Scientific Reports* **6:**23509. doi:

1051   10.1038/srep23509

1052 Furla, P., Galgani, I., Durand, I., and Allemand, D. 2000. Sources and mechanisms of inorganic

1053   carbon transport for coral calcification and photosynthesis. *Journal of Experimental Biology*

1054   **203**:3445-3457.

1055 Furuhashi, T., Beran, A., Blazso, M., Czegeny, Z., Schwarzinger, C., and Steiner, G. 2009. Pyrolysis

1056   GC/MS and IR spectroscopy in chitin analysis of molluscan shells. *Bioscience,*

1057   *biotechnology, and biochemistry* **73**:93-103.

1058 Gao, K., Ruan, Z., Villafañe, V.E., Gattuso, J.-P., and Helbling, E.W. 2009. Ocean acidification

1059   exacerbates the effect of UV radiation on the calcifying phytoplankter *Emiliania huxleyi*.

1060   *Limnology and Oceanography* **54**:1855-1862.

1061 Gazeau, F., Quiblier, C., Jansen, J.M., Gattuso, J.-P., Middelburg, J.J., and Heip, C.H.R. 2007. Impact

1062   of elevated CO_2 on shellfish calcification. *Geophysical Research Letters* **34**(7): L07603.

1063 Ghosh, P., Adkins, J., Affek, H., Balta, B., Guo, W., Schauble, E.A., Schrag, D., and Eiler, J.M. 2006.

1064   13C–18O bonds in carbonate minerals: A new kind of paleothermometer. *Geochimica et*

1065   *Cosmochimica Acta* **70**:1439-1456.

1066   Glas, M.S., Fabricius, K.E., de Beer, D., and Uthicke, S. 2012a. The O_2, pH and Ca^{2+}

1067   microenvironment of benthic foraminifera in a high CO_2 world. *PLOS ONE* **7**:e50010.

1068   doi:10.1371/journal.pone.0050010

1069   Glas, M.S., Langer, G., and Keul, N. 2012b. Calcification acidifies the microenvironment of a benthic

1070   foraminifer (Ammonia sp.). *Journal of Experimental Marine Biology and Ecology* **424-**

1071   **425**:53-58.

1072   Goffredo, S., Prada, F., Caroselli, E., Capaccioni, B., Zaccanti, F., Pasquini, L., Fantazzini, P.,

1073   Fermani, S., Reggi, M., Levy, O., Fabricius, K.E., Dubinsky, Z., and Falini, G. 2014.

1074   Biomineralization control related to population density under ocean acidification. *Nature*

1075   *Clim. Change* **4**:593-597.

1076   Gong, Y.U.T., Killian, C.E., Olson, I.C., Appathurai, N.P., Amasino, A.L., Martin, M.C., Holt, L.J.,

1077   Wilt, F.H., and Gilbert, P.U.P.A. 2012. Phase transitions in biogenic amorphous calcium

1078   carbonate. *PNAS* **109**:6088-6093.

1079   Guidetti, P., and Mori, M. 2005. Morpho-functional defences of Mediterranean sea urchins,

1080   *Paracentrotus lividus* and *Arbacia lixula*, against fish predators. *Marine Biology* **147**:797-

1081   802.

1082   Guo, W., Mosenfelder, J.L., Goddard III, W.A., and Eiler, J.M. 2009. Isotopic fractionations

1083   associated with phosphoric acid digestion of carbonate minerals: Insights from first-principles

1084   theoretical modeling and clumped isotope measurements. *Geochimica et Cosmochimica Acta*

1085   **73**:7203–7225.

1086   Hahn, S., Rodolfo-Metalpa, R., Griesshaber, E., Schmahl, W.W., Buhl, D., Hall-Spencer, J.M.,

1087   Baggini, C., Fehr, K.T., and Immenhauser, A. 2012. Marine bivalve shell geochemistry and

1088   ultrastructure from modern low pH environments: environmental effect versus experimental

1089   bias. *Biogeosciences* **9**:1897-1914.

1090   Harney, E., Artigaud, S., Le Souchu, P., Miner, P., Corporeau, C., Essid, H., Pichereau, V., and

1091   Nunes, F.L.D. 2016. Non-additive effects of ocean acidification in combination with warming

1092   on the larval proteome of the Pacific oyster, *Crassostrea gigas*. *Journal of proteomics*

1093   **135**:151-161.

1094   Hemming, N.G., and Hanson, G.N. 1992. Boron isotopic composition and concentration in modern

1095   marine carbonates. *Geochimica et Cosmochimica Acta* **56**:537-543.

1096   Herler, J., and Dirnwöber, M. 2011. A simple technique for measuring buoyant weight increment of

1097   entire, transplanted coral colonies in the field. *Journal of Experimental Marine Biology and*

1098   *Ecology* **407**:250-255.

1099   Hofmann, G.E., O'Donnell, M.J., and Todgham, A.E. 2008. Using functional genomics to explore the

1100   effects of ocean acidification on calcifying marine organisms. *Marine Ecology Progress*

1101   *Series* **373**:219-226.

1102   Huang, S., Chaudhary, K., and Garmire, L.X. 2017. More is better: recent progress in multi-omics

1103   data integration methods. *Frontiers in Genetics* **8**(84):1-12. doi:

1104   https://doi.org/10.3389/fgene.2017.00084

1105   Iglesias-Rodriguez, M.D., Halloran, P.R., Rickaby, R.E.M., Hall, I.R., Colmenero-Hidalgo, E.,

1106   Gittins, J.R., Green, D.R.H., Tyrrell, T., Gibbs, S.J., von Dassow, P., Rehm, E., Armbrust,

1107   E.V., and Boessenkool, K.P. 2008. Phytoplankton calcification in a high-CO_2 world. *Science*

1108   **320**:336-340.

1109   Jeffree, R.A., Markich, S.J., Lefebvre, F., Thellier, M., and Ripoll, C. 1995. Shell microlaminations of

1110   the freshwater bivalveHyridella depressa as an archival monitor of manganese water

1111   concentration: Experimental investigation by depth profiling using secondary ion mass

1112   spectrometry (SIMS). *Experientia* **51**:838-848.

1113   Jokiel, P.L., Rodgers, K.S., Kuffner, I.B., Andersson, A.J., Cox, E.F., and Mackenzie, F.T. 2008.

1114   Ocean acidification and calcifying reef organisms: a mesocosm investigation. *Coral Reefs*

1115   **27**:473-483.

1116   Joubert, C., Piquemal, D., Marie, B., Manchon, L., Pierrat, F., Zanella-Cléon, I., Cochennec-Laureau,

1117   N., Gueguen, Y., and Montagnani, C. 2010. Transcriptome and proteome analysis of Pinctada

1118   margaritifera calcifying mantle and shell: focus on biomineralization. *Bmc Genomics* **11**:613.

1119   Kamenos, N.A., Burdett, H.L., Aloisio, E., Findlay, H.S., Martin, S., Longobone, C., Dunn,

1120   J.Widdicombe, S., and Calosi, P. 2013. Coralline algal structure is more sensitive to rate,

1121   rather than the magnitude, of ocean acidification. *Global Change Biology* **19**:3621–3628.

1122 Katano, H., Takakuwa, M., Hayakawa, H., and Kimoto, H. 2016. Determination of chitin based on the

1123   colorimetric assay of glucosamine in acid hydrolysate. *Analytical Sciences.* **32**: 701-703.

1124 Keul, N., Langer, G., de Nooijer, L.J., Nehrke, G., Reichart, G.J., and Bijma, J. 2013. Incorporation of

1125   uranium in benthic foraminiferal calcite reflects seawater carbonate ion concentration.

1126   *Geochemistry, Geophysics, Geosystems* **14**:102-111.

1127 Khalifa, G.M., Kirchenbuechler, D., Koifman, N., Kleinerman, O., Talmon, Y., Elbaum, M., Addadi,

1128   L., Weiner, S., and Erez, J. 2016. Biomineralization pathways in a foraminifer revealed using

1129   a novel correlative cryo-fluorescence–SEM–EDS technique. *Journal of structural biology*

1130   **196**:155-163.

1131 Kikuchi, S. 1928. Diffraction of cathode rays by mica. *Proceedings of the Imperial Academy* **4**:354-

1132   356.

1133 Krief, S., Hendy, E.J., Fine, M., Yam, R., Meibom, A., Foster, G.L., and Shemesh, A. 2010.

1134   Physiological and isotopic responses of scleractinian corals to ocean acidification.

1135   *Geochimica et Cosmochimica Acta* **74**:4988-5001.

1136 Kruzic, J.J., Kim, D.K., Koester, K.J., and Ritchie, R.O. 2009. Indentation techniques for evaluating

1137   the fracture toughness of biomaterials and hard tissues. *Journal of the Mechanical Behavior*

1138   *of Biomedical Materials* **2**:384-395.

1139 Kunitake, M.E., Baker, S.P., and Estroff, L.A. 2012. The effect of magnesium substitution on the

1140   hardness of synthetic and biogenic calcite. *MRS Communications* **2**:113-116.

1141 Kunitake, M.E., Mangano, L.M., Peloquin, J.M., Baker, S.P., and Estroff, L.A. 2013. Evaluation of

1142   strengthening mechanisms in calcite single crystals from mollusk shells. *Acta Biomaterialia*

1143   **9**:5353-5359.

1144 Langdon, C., and Atkinson, M.J. 2005. Effect of elevated pCO$_2$ on photosynthesis and calcification of

1145   corals and interactions with seasonal change in temperature/irradiance and nutrient

1146   enrichment. *Journal of Geophysical Research: Oceans* **110**:C09S07.

1147 Langdon, C., Takahashi, T., Sweeney, C., Chipman, D., Goddard, J., Marubini, F., Aceves, H.,

1148   Barnett, H., and Atkinson, M.J. 2000. Effect of calcium carbonate saturation state on the

1149   calcification rate of an experimental coral reef. *Global Biogeochemical Cycles* **14**:639-654.

1150 Langer, G., Nehrke, G., Baggini, C., Rodolfo-Metalpa, R., Hall-Spencer, J.M., and Bijma, J. 2014.

1151 Limpets counteract ocean acidification induced shell corrosion by thickening of aragonitic

1152 shell layers. *Biogeosciences* **11**:7363-7368.

1153 Lawn, B.R., Evans, A., and Marshall, D. 1980. Elastic/plastic indentation damage in ceramics: the

1154 median/radial crack system. *Journal of the American Ceramic Society* **63**:574-581.

1155 Lear, C.H., Elderfield, H., and Wilson, P.A. 2000. Cenozoic deep-sea temperatures and global ice

1156 volumes from Mg/Ca in benthic foraminiferal calcite. *Science* **287**:269-272.

1157 Lee, C.G., Da Silva, C.A., Dela Cruz, C.S., Ahangari, F., Ma, B., Kang, M.J., He, C.H., Takyar, S.,

1158 and Elias, J.A. 2011. Role of chitin and chitinase/chitinase-like proteins in inflammation,

1159 tissue remodeling, and injury. *Annual Review of Physiology* **73**:479-501.

1160 Leung, J.Y., Russell, B.D., and Connell, S.D. 2017. Mineralogical plasticity acts as a compensatory

1161 mechanism to the impacts of ocean acidification. *Environmental science & technology*

1162 **51**(5):2652-2659.

1163 Levi-Kalisman, Y., Falini, G., Addadi, L., and Weiner, S. 2001. Structure of the nacreous organic

1164 matrix of a bivalve mollusk shell examined in the hydrated state using cryo-TEM. *Journal of*

1165 *structural biology* **135**:8-17.

1166 Lewis, B., and Diaz-Pulido, G. 2017. Suitability of three fluorochrome markers for obtaining in situ

1167 growth rates of coralline algae. *Journal of Experimental Marine Biology and Ecology* **490**:64-

1168 73.

1169 Li, C., Chan, V.B.S., He, C., Meng, Y., Yao, H., Shih, K., and Thiyagarajan, V. 2014. Weakening

1170 mechanisms of the serpulid tube in a high-CO_2 world. *Environmental science & technology*

1171 **48**:14158-14167.

1172 Li, C., Meng, Y., He, C., Chan, V.B.S., Yao, H., and Thiyagarajan, V. 2016. Mechanical robustness

1173 of the calcareous tubeworm *Hydroides elegans*: warming mitigates the adverse effects of

1174 ocean acidification. *Biofouling* **32**:191-204.

1175 Li, Y., Zhuang, S., Wu, Y., Ren, H., Cheng, F., Lin, X., Wang, K., Beardall, J., and Gao, K. 2015.

1176 Ocean acidification modulates expression of genes and physiological performance of a marine

1177 diatom. *Biogeosciences Discuss.* **2015**:15809-15833.

1178 Limbeck, A., Bonta, M., and Nischkauer, W. 2017. Improvements in the direct analysis of advanced

1179   materials using ICP-based measurement techniques. *Journal of Analytical Atomic*

1180   *Spectrometry* **32**:212-232.

1181 Lombardi, C., Cocito, S., Gambi, M.C., and Taylor, P.D. 2015. Morphological plasticity in

1182   a calcifying modular organism: evidence from an *in situ* transplant experiment in a natural

1183 CO_2 vent system. *Royal Society Open Science* **2**(2):140413. doi: 10.1098/rsos.140413.

1184 Luo, Y.-J., Takeuchi, T., Koyanagi, R., Yamada, L., Kanda, M., Khalturina, M., Fujie, M., Yamasaki,

1185   S.-I., Endo, K., and Satoh, N. 2015. The *Lingula* genome provides insights into brachiopod

1186   evolution and the origin of phosphate biomineralization. *Nature Communications* **6**: 8301.

1187   doi: 10.1038/ncomms9301

1188 Mackenzie, C.L., Ormondroyd, G.A., Curling, S.F., Ball, R.J., Whiteley, N.M., and Malham, S.K.

1189   2014. Ocean warming, more than acidification, reduces shell strength in a commercial

1190   shellfish species during food limitation. *PLOS ONE* **9**:e86764.

1191   doi:10.1371/journal.pone.0086764

1192 Mann, M., and Jensen, O.N. 2003. Proteomic analysis of post-translational modifications. *Nature*

1193   *biotechnology* **21**:255-261.

1194 Marie, B., Le Roy, N., Zanella-Cléon, I., Becchi, M., and Marin, F. 2011. Molecular evolution of

1195   mollusc shell proteins: insights from proteomic analysis of the edible mussel *Mytilus*. *Journal*

1196   *of molecular evolution* **72**:531-546.

1197 Marie, B., Marie, A., Jackson, D.J., Dubost, L., Degnan, B.M., Milet, C., and Marin, F. 2010.

1198   Proteomic analysis of the organic matrix of the abalone *Haliotis asinina* calcified shell.

1199   *Proteome Science* **8**:54. doi: 10.1186/1477-5956-8-54

1200 Marsh, J.A. 1970. Primary Productivity of Reef-Building Calcareous Red Algae. *Ecology* **51**:255-263.

1201 Martin, P., Goodkin, N.F., Stewart, J.A., Foster, G.L., Sikes, E.L., White, H.K., Hennige, S., and

1202   Roberts, J.M. 2016. Deep-sea coral δ13C: A tool to reconstruct the difference between

1203   seawater pH and δ11B-derived calcifying fluid pH. *Geophysical Research Letters* **43**:299-

1204   308.

1205   Martin, P.A., and Lea, D.W. 2002. A simple evaluation of cleaning procedures on fossil benthic

1206   foraminiferal Mg/Ca. *Geochemistry, Geophysics, Geosystems* **3**:1-8.

1207   Marxen, J.C., Nimtz, M., Becker, W., and Mann, K. 2003. The major soluble 19.6 kDa protein of the

1208   organic shell matrix of the freshwater snail *Biomphalaria glabrata* is an N-glycosylated

1209   dermatopontin. *Biochimica et Biophysica Acta (BBA)-Proteins and Proteomics* **1650**:92-98.

1210   McConnaughey, T.A., and Gillikin, D.P. 2008. Carbon isotopes in mollusk shell carbonates. *Geo-*

1211   *Marine Letters* **28**:287-299.

1212   McEnery, M., and Lee, J.J. 1970. Tracer studies on calcium and strontium mineralization and mineral

1213   cycling in two species of foraminifera, *Rosalina leei* and *Spiroloculina hyalina. Limnology*

1214   *and Oceanography* **15**:173-182.

1215   Melbourne, L.A., Griffin, J., Schmidt, D.N., and Rayfield, E.J.. 2015. Potential and limitations of

1216   finite element modelling in assessing structural integrity of coralline algae under future global

1217   change. *Biogeosciences.* **12**(15): 5891-5883. doi: 10.5194/bg-12-5871-2015

1218   Melzner, F., Stange, P., Trubenbach, K., Thomsen, J., Casties, I., Panknin, U., Gorb, S.N., and

1219   Gutowska, M.A. 2011. Food supply and seawater pCO$_2$ impact calcification and internal shell

1220   dissolution in the blue mussel *Mytilus edulis. PLOS ONE* **6**:e24223. doi:

1221   10.1371/journal.pone.0024223

1222   Milano, S., Schöne, B.R., Wang, S., and Müller, W.E. 2016. Impact of high pCO$_2$ on shell structure of

1223   the bivalve *Cerastoderma edule. Marine Environmental Research* **119**:144-155.

1224   Milazzo, M., Rodolfo-Metalpa, R., Chan, V.B.S., Fine, M., Alessi, C., Thiyagarajan, V., Hall-

1225   Spencer, J.M., and Chemello, R. 2014. Ocean acidification impairs vermetid reef recruitment.

1226   *Scientific Reports* **4**:4189.

1227   Miyamoto, H., Miyashita, T., Okushima, M., Nakano, S., Morita, T., and Matsushiro, A. 1996. A

1228   carbonic anhydrase from the nacreous layer in oyster pearls. *Proceedings of the National*

1229   *Academy of Sciences* **93**:9657-9660.

1230   Molina, R., Hanlon, S., Savidge, T., Bogan, A., and Levine, J. 2005. Buoyant weight technique:

1231   application to freshwater bivalves. *American Malacological Bulletin* **20**:49-53.

1232 Müller, M.N., Kısakürek, B., Buhl, D., Gutperlet, R., Kolevica, A., Riebesell, U., Stoll, H., and

1233   Eisenhauer, A. 2011. Response of the coccolithophores *Emiliania huxleyi* and *Coccolithus*

1234   *braarudii* to changing seawater Mg^{2+} and Ca^{2+} concentrations: Mg/Ca, Sr/Ca ratios and

1235   δ44/40Ca, δ26/24Mg of coccolith calcite. *Geochimica et Cosmochimica Acta* **75**:2088-2102.

1236 Naddafi, R., and Rudstam, L.G. 2014. Predator induced morphological change in dreissenid mussels:

1237   implications for species replacement. *Freshwater Biology* **59**:703-713.

1238 Nakayama, S., Suzuki, M., Endo, H., Limura, K., Kinoshita, S., Watabe, S., Kogure, T., and

1239   Nagasawa, H. 2013. Identification and characterization of a matrix protein (PPP-10) in the

1240   periostracum of the pearl oyster, *Pinctada fucata*. *FEBS open bio* **3**:421-427.

1241 Nellist, P.D., Chisholm, M.F., Dellby, N., Krivanek, O.L., Murfitt, M.F., Szilagyi, Z.S., Lupini, A.R.,

1242   Borisevich, A., Sides, W.H., and Pennycook, S.J. 2004. Direct sub-angstrom imaging of a

1243   crystal lattice. *Science* **305**:1741-1741.

1244 Newbury, D.E. 1998. Trace element detection at nanometer scale spatial resolution. *Microscopy*

1245   **47**:407-418.

1246 Nimer, N.A., and Merrett, M.J. 1993. Calcification rate in *Emiliania huxleyi* Lohmann in response to

1247   light, nitrate and availability of inorganic carbon. *New Phytologist* **123**:673-677.

1248 Nishikawa, S., and Kikuchi, S. 1928. Diffraction of cathode rays by calcite. *Nature* **122**:726-726.

1249 Norzagaray-López, O.C., Calderon-Aguilera, L.E., Castro-Ceseña, A.B., Hirata, G., and Hernández-

1250   Ayón, J.M. 2017. Skeletal dissolution kinetics and mechanical tests in response to

1251   morphology among coral genera. *Facies* **63**:7. doi: 10.1007/s10347-016-0488-2

1252 Not, C., Thibodeau, B., and Yokoyama, Y. 2018. Incorporation of Mg, Sr, Ba, U, and B in high-Mg

1253   calcite benthic foraminifers cultured under controlled pCO$_2$. *Geochemistry, Geophysics,*

1254   *Geosystems* **19**:83-98.

1255 Nudelman, F, Chen, H.H., Goldberg, H.A., Weiner, S., Addadi, L. 2007. Spiers Memorial Lecture.

1256   Lessons from biomineralization: comparing the growth strategies of mollusc shell prismatic

1257   and nacreous layers in *Atrina rigida*. *Faraday Discuss* **136**:9-25.

1258   Nürnberg, D., Bijma, J., and Hemleben, C. 1996. Assessing the reliability of magnesium in

1259   foraminiferal calcite as a proxy for water mass temperatures. *Geochimica et Cosmochimica*

1260   *Acta* **60**:803-814.

1261   Oliver, W.C., and Pharr, G.M. 1992. An improved technique for determining hardness and elastic

1262   modulus using load and displacement sensing indentation experiments. *Journal of Materials*

1263   *Research* **7**:1564-1583.

1264   Orr, J.C., Fabry, V.J., Aumont, O., Bopp, L., Doney, S.C., Feely, R.A., Gnanadesikan, A., Gruber, N.,

1265   Ishida, A., and Joos, F. 2005. Anthropogenic ocean acidification over the twenty-first century

1266   and its impact on calcifying organisms. *Nature* **437**:681-686.

1267   Paasche, E. 1963. The adaptation of the carbon-14 method for the measurement of coccolith

1268   production in *Coccolithus huxleyi*. *Physiologia Plantarum* **16**:186-200.

1269   Pan, T.C.F., Applebaum, S.L., and Manahan, D.T. 2015. Experimental ocean acidification alters the

1270   allocation of metabolic energy. *Proceedings of the National Academy of Sciences* **112**:4696-

1271   4701.

1272   Parkinson, D., Curry, G.B., Cusack, M., and Fallick, A.E. 2005. Shell structure, patterns and trends of

1273   oxygen and carbon stable isotopes in modern brachiopod shells. *Chemical Geology* **219**:193-

1274   235.

1275   Pearson, F., Marchessault, R., and Liang, C. 1960. Infrared spectra of crystalline polysaccharides. V.

1276   Chitin. *Journal of Polymer Science* **43**:101-116.

1277   Perez-Huerta, A., and Cusack, M. 2009. Optimizing electron backscatter diffraction of carbonate

1278   biominerals-resin type and carbon coating. *Microscopy and Microanalysis* **15**:197-203.

1279   Pérez-Huerta, A., Cusack, M., Jeffries, T.E., and Williams, C.T. 2008. High resolution distribution of

1280   magnesium and strontium and the evaluation of Mg/Ca thermometry in Recent brachiopod

1281   shells. *Chemical Geology* **247**:229-241.

1282   Politi, Y., Levi-Kalisman, Y., Raz, S., Wilt, F., Addadi, L., Weiner, S., and Sagi, I. 2006. Structural

1283   characterization of the transient amorphous calcium carbonate precursor phase in sea urchin

1284   embryos. *Advanced Functional Materials* **16**:1289-1298.

1285 Politi, Y., Metzler, R.A., Abrecht, M., Gilbert, B., Wilt, F.H., Sagi, I., Addadi, L., Weiner, S., and
1286   Gilbert, P.U.P.A. 2008. Transformation mechanism of amorphous calcium carbonate into
1287   calcite in the sea urchin larval spicule. *Proceedings of the National Academy of Sciences of*
1288   *the United States of America* **105**:17362-17366.

1289 Rae, J.W.B., Foster, G.L., Schmidt, D.N., and Elliott, T. 2011. Boron isotopes and B/Ca in benthic
1290   foraminifera: Proxies for the deep ocean carbonate system. *Earth and Planetary Science*
1291   *Letters* **302**:403-413.

1292 Ragazzola, F., Foster, L.C., Form, A., Anderson, P.S.L., Hansteen, T.H., and Fietzke, J. 2012. *Global*
1293   *Change Biology.* **18**(9): 2804-2812. doi: 10.1111/j.1365-2486.2012.02756.x

1294 Reynaud, S., Leclercq, N., Romaine-Lioud, S., Ferrier-Pages, C., Jaubert, J., and Gattuso, J. P. 2003.
1295   Interacting effects of CO_2 partial pressure and temperature on photosynthesis and calcification
1296   in a scleractinian coral. *Global Change Biology* **9**:1660-1668.

1297 Riebesell, U., Zondervan, I., Rost, B., Tortell, P.D., Zeebe, R.E., and Morel, F.M.M. 2000. Reduced
1298   calcification of marine plankton in response to increased atmospheric CO_2. *Nature* **407**:364-
1299   367.

1300 Ries, J.B., Cohen, A.L., and McCorkle, D.C. 2009. Marine calcifiers exhibit mixed responses to CO_2-
1301   induced ocean acidification. *Geology* **37**:1131-1134.

1302 Rodolfo-Metalpa, R., Houlbreque, F., Tambutte, E., Boisson, F., Baggini, C., Patti, F.P., Jeffree, R.,
1303   Fine, M., Foggo, A., Gattuso, J.P., and Hall-Spencer, J.M. 2011. Coral and mollusc resistance
1304   to ocean acidification adversely affected by warming. *Nature Clim. Change* **1**:308-312.

1305 Rodolfo-Metalpa, R., Montagna, P., Aliani, S., Borghini, M., Canese, S., Hall-Spencer, J.M., Foggo,
1306   A., Milazzo, M., Taviani, M., and Houlbrèque, F. 2015. Calcification is not the Achilles' heel
1307   of cold-water corals in an acidifying ocean. *Global Change Biology* **21**:2238-2248.

1308 Roleda, M.Y., Boyd, P.W., and Hurd, C.L. 2012. Before ocean acidification: calcifier chemistry
1309   lessons. *Journal of Phycology* **48**:840-843.

1310 Rühl, S., Calosi, P., Faulwetter, S., Keklikoglou, K., Widdicombe, S., and Queirós, A.M. 2017. Long-
1311   term exposure to elevated $p$$CO_2$ more than warming modifies early-life shell growth in a
1312   temperate gastropod. *ICES Journal of Marine Science* **74**:1113-1124.

1313 Sabatier, P., Reyss, J.L., Hall-Spencer, J.M., Colin, C., Frank, N., Tisnérat-Laborde, N., Bordier, L.,

1314   and Douville, E. 2012. ^{210}Pb-^{226}Ra chronology reveals rapid growth rate of *Madrepora*

1315   *oculata* and *Lophelia pertusa* on world's largest cold-water coral reef. *Biogeosciences* **9**:1253-

1316   1265.

1317 Samata, T., Hayashi, N., Kono, M., Hasegawa, K., Horita, C., and Akera, S. 1999. A new matrix

1318   protein family related to the nacreous layer formation of *Pinctada fucata*. *FEBS letters*

1319   **462**:225-229.

1320 Satoh, M., Iwamoto, K., Suzuki, I., and Shiraiwa, Y. 2009. Cold stress stimulates intracellular

1321   calcification by the coccolithophore, *Emiliania huxleyi* (Haptophyceae) under phosphate-

1322   deficient conditions. *Marine biotechnology* **11**:327-333.

1323 Schoepf, V., Hu, X., Holcomb, M., Cai, W.J., Li, Q., Wang, Y., Xu, H., Warner, M.E., Melman, T.F.,

1324   Hoadley, K.D., Pettay, D.T., Matsui, Y., Baumann, J.H., and Grottoli, A.G. 2017. Coral

1325   calcification under environmental change: a direct comparison of the alkalinity anomaly and

1326   buoyant weight techniques. *Coral Reefs* **36**:13-25.

1327 Sikes, C.S., Wheeler, A.P., Wierzbicki, A., Mount, A.S., and Dillaman, R.M. 2000. Nucleation and

1328   growth of calcite on native versus pyrolyzed oyster shell folia. *Biological Bulletin* **198**:50-66.

1329 Sinclair, D.J. 2005. Correlated trace element "vital effects" in tropical corals: A new geochemical tool

1330   for probing biomineralization. *Geochimica et Cosmochimica Acta* **69**:3265-3284.

1331 Singh, S.K., and Sigworth, F.J. 2015. Cryo-EM: Spinning the Micelles Away. *Structure* **23**:1561. doi:

1332   10.1016/j.str.2015.08.001

1333 Spero, H.J., Bijma, J., Lea, D.W., and Bemis, B.E. 1997. Effect of seawater carbonate concentration

1334   on foraminiferal carbon and oxygen isotopes. *Nature* **390**:497-500.

1335 Stewart, J.A., Anagnostou, E., and Foster, G.L. 2016. An improved boron isotope pH proxy

1336   calibration for the deep-sea coral *Desmophyllum dianthus* through sub-sampling of fibrous

1337   aragonite. *Chemical Geology* **447**:148-160.

1338 Stumpp, M., Hu, M.Y., Melzner, F., Gutowska, M.A., Dorey, N., Himmerkus, N., Holtmann, W.C.,

1339   Dupont, S.T., Thorndyke, M.C., and Bleich, M. 2012. Acidified seawater impacts sea urchin

1340   larvae pH regulatory systems relevant for calcification. *Proceedings of the National Academy*

1341   *of Sciences* **109**:18192-18197.

1342 Suzuki, M., Iwashima, A., Tsutsui, N., Ohira, T., Kogure, T., and Nagasawa, H. 2011. Identification

1343   and characterisation of a calcium carbonate-binding protein, blue mussel shell protein

1344   (BMSP), from the nacreous layer. *Chembiochem* **12**:2478-2487.

1345 Suzuki, M., Murayama, E., Inoue, H., Ozaki, N., Tohse, H., Kogure, T., and Nagasawa, H. 2004.

1346   Characterization of Prismalin-14, a novel matrix protein from the prismatic layer of the

1347   Japanese pearl oyster (*Pinctada fucata*). *Biochemical Journal* **382**:205-213.

1348 Suzuki, M., and Nagasawa, H. 2013. Mollusk shell structures and their formation mechanism.

1349   *Canadian Journal of Zoology* **91**:349-366.

1350 Suzuki, M., Sakuda, S., and Nagasawa, H. 2007. Identification of chitin in the prismatic layer of the

1351   shell and a chitin synthase gene from the Japanese pearl oyster, *Pinctada fucata. Bioscience,*

1352   *biotechnology, and biochemistry* **71**:1735-1744.

1353 Suzuki, M., Saruwatari, K., Kogure, T., Yamamoto, Y., Nishimura, T., Kato, T., and Nagasawa, H.

1354   2009. An acidic matrix protein, Pif, is a key macromolecule for nacre formation. *Science*

1355   **325**:1388-1390.

1356 Takeuchi, T., Kawashima, T., Koyanagi, R., Gyoja, F., Tanaka, M., Ikuta, T., Shoguchi, E., Fujiwara,

1357   M., Shinzato, C., and Hisata, K. 2012. Draft genome of the pearl oyster *Pinctada fucata*: a

1358   platform for understanding bivalve biology. *DNA research*: **19**(2):117-30. doi:

1359   10.1093/dnares/dss005

1360 Tambutté, E., Tambutté, S., Segonds, N., Zoccola, D., Venn, A., Erez, J., and Allemand, D. 2012.

1361   Calcein labelling and electrophysiology: insights on coral tissue permeability and

1362   calcification. *Proceedings of the Royal Society B: Biological Sciences* **279**:19-27.

1363 Tambutté, E., Venn, A.A., Holcomb, M., Segonds, N., Techer, N., Zoccola, D., Allemand, D., and

1364   Tambutté, S. 2015. Morphological plasticity of the coral skeleton under CO_2-driven seawater

1365   acidification. *Nature Communications* **6**:7368. doi: 10.1038/ncomms8368

Taylor, J.R.A., Gilleard, J.M., Allen, M.C., and Deheyn, D.D. 2015. Effects of CO_2-induced pH reduction on the exoskeleton structure and biophotonic properties of the shrimp Lysmata californica. *Scientific Reports* **5**:10608. doi: 10.1038/srep10608

Taylor, P.D., Tan A.S.H., Kudryavstev, A.B., and Schopf, J.W. 2016. Carbonate mineralogy of a tropical bryozoan biota and its vulnerability to ocean acidification. *Marine Biology Research* **12**:776-780.

ter Kuile, B., Erez, J., and Padan, E. 1989. Mechanisms for the uptake of inorganic carbon by two species of symbiont-bearing foraminifera. *Marine Biology* **103**:241-251.

Thompson, R.F., Walker, M., Siebert, C.A., Muench, S.P., and Ranson, N.A. 2016. An introduction to sample preparation and imaging by cryo-electron microscopy for structural biology. *Methods* **100**:3-15.

Thor, P., and Dupont, S. 2015. Transgenerational effects alleviate severe fecundity loss during ocean acidification in a ubiquitous planktonic copepod. *Global Change Biology* **21**:2261-2271.

Titze, B., and Genoud, C. 2016. Volume scanning electron microscopy for imaging biological ultrastructure. *Biology of the Cell* **108**:307-323.

Todgham, A.E., and Hofmann, G.E. 2009. Transcriptomic response of sea urchin larvae Strongylocentrotus purpuratus to CO_2-driven seawater acidification. *Journal of Experimental Biology* **212**:2579-2594.

Toyofuku, T., Matsuo, M.Y., De Nooijer, L.J., Nagai, Y., Kawada, S., Fujita, K., Reichart, G.J., Nomaki, H., Tsuchiya, M., and Sakaguchi, H. 2017. Proton pumping accompanies calcification in foraminifera. *Nature Communications* **8**:14145. doi: 10.1038/ncomms14145

Venn, A., Tambutté, E., Holcomb, M., Allemand, D., and Tambutté, S. 2011. Live tissue imaging shows reef corals elevate pH under their calcifying tissue relative to seawater. *PLOS ONE* **6**:e20013. doi: 10.1371/journal.pone.0020013

Venn, A.A., Tambutté, E., Holcomb, M., Laurent, J., Allemand, D., and Tambutté, S. 2013. Impact of seawater acidification on pH at the tissue–skeleton interface and calcification in reef corals. *Proceedings of the National Academy of Sciences* **110**:1634-1639.

1393   Vézina, A.F., and Hoegh-Guldberg, O. 2008. Introduction: Effects of ocean acidification on marine

1394   ecosystems. *Marine Ecology Progress Series* **373**:199-201.

1395   Von Euw, S., Zhang, Q., Manichev, V., Murali, N., Gross, J., Feldman, L.C., Gustafsson, T., Flach,

1396   C., Mendelsohn, R., and Falkowski, P.G. 2017. Biological control of aragonite formation in

1397   stony corals. *Science* **356**:933-938.

1398   Wall, M., Fietzke, J., Schmidt, G.M., Fink, A., Hofmann, L.C., de Beer, D., and Fabricius, K.E. 2016.

1399   Internal pH regulation facilitates in situ long-term acclimation of massive corals to end-of-

1400   century carbon dioxide conditions. *Scientific Reports* **6**:30688. doi: 10.1038/srep30688

1401   Wang, X., Wang, M., Xu, J., Jia, Z., Liu, Z., Wang, L., and Song, L. 2017. Soluble adenylyl cyclase

1402   mediates mitochondrial pathway of apoptosis and ATP metabolism in oyster *Crassostrea*

1403   *gigas* exposed to elevated CO_2. *Fish & Shellfish Immunology* **66**:140-147.

1404   Watabe, N. 1965. Studies on shell formation: XI. Crystal—matrix relationships in the inner layers of

1405   mollusk shells. *Journal of ultrastructure research* **12**:351-370.

1406   Wehrmeister, U., Jacob, D.E., Soldati, A.L., Loges, N., Häger, T., and Hofmeister, W. 2011.

1407   Amorphous, nanocrystalline and crystalline calcium carbonates in biological materials.

1408   *Journal of Raman Spectroscopy* **42**:926-935.

1409   Wei, L., Wang, Q., Wu, H., Ji, C., and Zhao, J. 2015. Proteomic and metabolomic responses of

1410   Pacific oyster Crassostrea gigas to elevated pCO_2 exposure. *Journal of proteomics* **112**:83-94.

1411   Weiner, S., and Dove, P.M. 2003. An Overview of Biomineralization Processes and the Problem of

1412   the Vital Effect. *Reviews in Mineralogy and Geochemistry* **54**:1-29.

1413   Weiner, S., and Traub, W. 1980. X-ray diffraction study of the insoluble organic matrix of mollusk

1414   shells. *FEBS letters* **111**:311-316.

1415   Weiss, I.M., and Schönitzer, V. 2006. The distribution of chitin in larval shells of the bivalve mollusk

1416   *Mytilus galloprovincialis*. *Journal of structural biology* **153**:264-277.

1417   Wiese, S., Reidegeld, K.A., Meyer, H.E., and Warscheid, B. 2007. Protein labeling by iTRAQ: A

1418   new tool for quantitative mass spectrometry in proteome research. *Proteomics* **7**:340-350.

1419   Wilbur, K.M. 1964. Shell formation and regeneration. *In* K.M. Wilbur and C.M. Younge, (eds).

1420   *Physiology and the mollusca*. Academic Press, New York. Pages 243-282.

1421 Wilkinson, B.H. 1979. Biomineralization, paleoceanography, and the evolution of calcareous marine

1422   organisms. *Geology* **7**:524-527.

1423 Williams, P. 1985. Secondary ion mass spectrometry. *Annual Review of Materials Science* **15**:517-

1424   548.

1425 Wittmann, A.C., and Pörtner, H.O. 2013. Sensitivities of extant animal taxa to ocean acidification.

1426   *Nature Climate Change* **3**:995-1001.

1427 Wolfe, K., Smith, A.M., Trimby, P., and Byrne, M. 2013. Microstructure of the paper nautilus

1428   (Argonauta nodosa) shell and the novel application of electron backscatter diffraction (EBSD)

1429   to address effects of ocean acidification. *Marine Biology* **160**:2271-2278.

1430 Wood, H.L., Spicer, J.I., and Widdicombe, S. 2008. Ocean acidification may increase calcification

1431   rates, but at a cost. *Proceedings of the Royal Society B: Biological Sciences* **275**:1767-1773.

1432 Yokoo, N., Suzuki, M., Saruwatari, K., Aoki, H., Watanabe, K., Nagasawa, H., and Kogure, T. 2011.

1433   Microstructures of the larval shell of a pearl oyster, *Pinctada fucata*, investigated by FIB-

1434   TEM technique. *American Mineralogist* **96**:1020-1027.

1435 Zhang, C., and Zhang, R. 2006. Matrix proteins in the outer shells of molluscs. *Marine biotechnology*

1436   **8**:572-586.

1437 Zhang, G., Fang, X., Guo, X., Li, L., Luo, R., Xu, F., Yang, P., Zhang, L., Wang, X., Qi, H., Xiong,

1438   Z., Que, H., Xie, Y., Holland, P.W., Paps, J., Zhu, Y., Wu, F., Chen, Y., Wang, J., Peng, C.,

1439   Meng, J., Yang, L., Liu, J., Wen, B., Zhang, N., Huang, Z., Zhu, Q., Feng, Y., Mount, A.,

1440   Hedgecock, D., Xu, Z., Liu, Y., Domazet-Lošo, T., Du, Y., Sun, X., Zhang, S., Liu, B.,

1441   Cheng, P., Jiang, X., Li, J., Fan, D., Wang, W., Fu, W., Wang, T., Wang, B., Zhang, J., Peng,

1442   Z., Li, Y., Li, N., Wang, J., Chen, M., He, Y., Tan, F., Song, X., Zheng, Q., Huang, R., Yang,

1443   H., Du, X., Chen, L., Yang, M., Gaffney, P.M., Wang, S., Luo, L., She, Z., Ming, Y., Huang,

1444   W., Zhang, S., Huang, B., Zhang, Y., Qu, T., Ni, P., Miao, G., Wang, J., Wang, Q., Steinberg,

1445   C.E., Wang, H., Li, N., Qian, L., Zhang, G., Li, Y., Yang, H., Liu, X., Wang, J., Yin, Y.,

1446   Wang, J. 2012. The oyster genome reveals stress adaptation and complexity of shell

1447   formation. *Nature* **490**:49-54.

1448   Zhang, S., Henehan, M.J., Hull, P.M., Reid, R.P., Hardisty, D.S., Hood, A.V.S., and Planavsky, N.J.

1449   2017. Investigating controls on boron isotope ratios in shallow marine carbonates. *Earth and*

1450   *Planetary Science Letters* **458**:380-393.

1451   Zhao, P., and Cai, W.J. 1999. pH polymeric membrane microelectrodes based on neutral carriers and

1452   their application in aquatic environments. *Anal. Chim Acta* **395**:285-291.

1453

1454

1455   **Table 1.** Summary of established techniques on Growth and Development to measure calcification and morphology under OA conditions with details of

1456   measurements, advantages and disadvantages of each application.

1457

1458   **Table 2.** Summary of emerging techniques on Mechanical tests to investigate mechanical properties under OA conditions with details of measurements,

1459   advantages and disadvantages of each application.

1460

1461   **Table 3.** Summary of emerging techniques on Mineral composition to investigate mechanical properties under OA conditions with details of measurements,

1462   advantages and disadvantages of each application.

1463

1464   **Table 4.** Summary of emerging techniques on Cellular biomineralization mechanisms to investigate mechanical properties under OA conditions with details

1465   of measurements, advantages and disadvantages of each application.

1466

1467

1468

1469

1. Growth and development			
Technique	*Measurement(s)*	*Advantages*	*Disadvantages*
Dyes - alizarin red and calcein	• Alizarin red stains calcium rich structures a red/light purple colour • Calcein stains calcium rich structures a fluorescent green colour	• Low cost, non-invasive • Track shell growth of living organisms during exposure to experiment • Data comparable to published work • Dye location can be analysed with advanced characterisation methods	• Alizarin red also binds free Ca • Calcein also binds Ca^{2+}, Mg^{2+}, Zn^{2+} • Is not compatible with other fluorescence techniques such as internal pH measurement • No mineral phase information
SEM	• High resolution characterisation • Ultrastructures of minerals	• Low cost • Data are comparable • Provide structural information	• No mineral phase information
Buoyant weight	• Mineral content determined from submerged weight of organism	• Low cost • Non-invasive • More accurate than length or area measurements • Mineral density changes are reflected in measurement	• Seawater density varies when temperature and salinity change • Purpose-made setup needed
Radioactive isotopes	• ^{45}Ca incorporation rate • ^{14}C incorporation • Represents mineralisation process during an experiment	• More accurate than length or area measurements • Synthetic isotopes are specific to the study	• Invasive acid digestion of mineral samples are needed for scintillation measurement • Requires handling of radioactive substances
Total alkalinity anomaly technique	• Alkalinity reduction surrounding an organism	• Low cost • Accurate	• Incubation in individual organism required

			• Not suitable for long-term studies
2. Mechanical tests - Protective function or ability to survive protection			
Technique	**Measurement(s)**	**Advantages**	**Disadvantages**
Three-point bending tests	• Elastic modulus • Fracture toughness	• Mimic predatory attack • Simple operation • Low cost	• Requires a tailor-made device • Test samples are cut into a standard size for testing
Computed tomography	• Shell thickness • Shell volume • Shell density	• 3D visualisation of shell shape for morphometric analysis	• Hard to detect planktonic and larval samples (15 - 1000 μm per pixel) • Standard density calibrated with bone mineral density (BMD, in g.cm^{-3})
Finite element analysis	• Visualize structural weakness of a material • Provide a numerical model for material properties	• Links nanoindentation data to whole sample measurements • Takes shell shape changes into account • Data can be verified by mechanical tests	• Requires computational skills • Shape information requires simpliflied experimental data • FEA Models need experimental verification
Microindentation	• Compressive force using 4- Vickers tip • Hardness • Elasticity Modulus	• Broader Vickers tip is less localised than nanoindentation • Lower cost than nanoindentation • Provides microscale spatial resolution	• Localised measurement • Does not represent shape and mechanical behaviour of the whole structure • Destructive to the sampling area of the specimen
Nanoindentation	• Compressive force using Berkovich tip • Hardness • Elasticity Modulus	• Sharper Berkovich tip enables higher spatial refinement of measurements • Provides both hardness and elasticity data in one measurement	• Localised measurement • Does not represent shape and mechanical behaviour of the whole structure • Destructive to the sampling area of the specimen

1470

1471

1472

3. Biomineralisation mechanisms to enable growth			
Elemental analysis			
Technique	**Measurement(s)**	**Advantages**	**Disadvantages**
Inductively coupled plasma (ICP) spectrometry	• Element to calcium ratios, e.g. Mg/Ca, Sr/Ca • Analyse acid digested samples	• Quantitative • Data are comparable • Coupling with OES, MS or AES provides different sensitivity at various costs	• Destructive sample preparation • Requires elemental standards • More sensitive instruments are more costly
laser ablation (LA)	• Element to calcium ratios, e.g. Mg/Ca, Sr/Ca • Analyse solid samples	• Spatial resolution • Less destructive than ICP approach • Data are comparable	• Spatial resolution of > 5 μm, less than SIMS • Less sensitive than ICP approach
Analytical electron microscopy (AEM) with energy dispersive X-ray spectrometry (EDS)	• Element to calcium ratios, e.g. Mg/Ca, Sr/Ca • Microanalysis provides a compositional map with spatial resolution	• Low cost and accessible • Spatial resolution • Non-destructive to specimen surface, therefore can be followed by EBSD, LA-ICP-MS or nanoindentation	• Requires elemental standards • Detection level at 1000 ppm
AEM with wavelength-dispersive X-ray spectroscopy (WDS)		• Moderate cost • Nanometer-scale resolution	• More costly than AEM-EDS
Structured illumination microscopy (SIMS)		• Spatial resolution of SEM • Detection sensitivity of 1ppm	• High cost • Destructive to the sampling area of the specimen

Electron energy loss spectrometry (EELS)		• 10 ppm detection limit • High resolution compositional map	• High cost • Require 10 nm thick samples • Small region of interest

1473

3. Biomineralisation mechanisms to enable growth (cont.)			
Mineral composition analyses			
Technique	Measurement(s)	Advantages	Disadvantages
Fourier transform infrared spectroscopy (FTIR)	• Intensity ratio $(I_{max}v_2/I_{max}v_4)$ between the absorption bands • Identifies the presence of aragonite or calcite	• Low cost • Provides a comparable measurement of ACC • Requires ~1 mg of mineral sample	• Semi-quantitative • No spatial resolution • Destructive
X-ray diffraction (XRD)	• Identifies the presence of aragonite or calcite	• Allows for quantification of calcite and aragonite ratios • Peak position suggests Mg content • Powdered sample can be acid-digested to provide elemental data	• Requires more powdered samples than FTIR • No spatial resolution • Destructive • Quantitative measurement requires the addition of CaF_2 as an internal standard
Raman spectroscopy	• Identifies the distribution of aragonite or calcite	• Spatial resolution • Area of calcite and aragonite is quantifiable • Specimen surface can be analysed by SEM and AEM methods for ultrastructure and elemental contents	• Requires sectional surfaces • Bleaching is necessary to remove organic contaminants • Limited spatial resolution
SEM-EBSD	• Identifies the distribution of calcite and aragonite	• Allows visual comparison of mineral crystals	• Requires fine polishing

	• High resolution crystallographic orientation data	• Provides quantifiable data on thickness of polymorphs • Spatial resolution	• Sectional axis and plane of observation must be standardised • Moderate cost

1474

1475

1476

3. Biomineralisation mechanisms to enable growth (cont.)			
Mineral composition analyses (cont.)			
Technique	Measurement(s)	Advantages	Disadvantages
X-ray photo emission electron microscopy (XPEEM) X-ray atomic spectroscopy (XAS) X-ray absorption near edge structure (XANES)	• High-spatial resolution composition map • Localises and characterises ACC • Identify mineral phases	• High spatial resolution • Sample preparation enables SEM observation and SEM-EBSD characterisation	• High cost • Requires fine polishing • Time-consuming
Atomic force microscopy (AFM)	• Records force-distance curve • Visualises fine topographical features	• Nanometre resolution • Simple sample preparation • Possible to measure hydrated samples in electrolyte solution	• High cost • Small area of interest • Time-consuming
Focused ion beam Transmission electron microscopy FIB-TEM	• Fine spatial resolution • FIB prepares TEM sections	• Selective region of interest • High spatial resolution • Suitable for small samples	• High cost • Time-consuming • Small area of interest

Cryo-electron microscopy	• High resolution study of biological sample after rapid freezing	• High resolution • Provides information on composition and crystallography	• High cost • Requires stabilising detergents for structure
Stable isotopes	• Detection of stable isotopes, e.g. $\delta13C$, $\delta18O$, 10B and $\delta11B$	• Data are comparable • Measures changes in metabolic activity in biomineralisation	• Destructive • Some proxies are not well established
Radioactive isotopes	• Calcification rate • Labelling with radioactive isotopes, e.g. ^{45}Ca and ^{14}C	• Sensitive technique • Specific to experimental exposure	• Continual spiking of radiotracer required during incubation • Destructive

1477
1478

4. Cellular biomineralization mechanisms			
Technique	**Measurement(s)**	**Advantages**	**Disadvantages**
SDS-PAGE and MS	• Characterises shell proteins	• Established protocol for protein identification • Low cost and high throughput of samples	• Sensitivity insufficient to detect shell proteins occurring at low quantity • Protein extraction and purification is time consuming • Difficult to interpret sequences from non-model marine organisms
Insoluble organic component analysis using X-ray diffraction (XRD)	• Characteristic spectroscopy correlated to chitin	• Provides evidence on the presence of chitin • Analyses insoluble solid samples	• Destructive • Sufficient sample is hard to obtain • Information has poor relevance to the cells and tissue associate with chitin
Insoluble organic component analysis using infra-red (IR) spectroscopy			

Pyrolysis NMR gas chromatography–mass spectrometry (GC-MS)	• Detects decomposition product of chitin after chitinase action	• Analyses the digested products • Digested product peaks can be quantified and compared	• Requires chemical standards of digested products • Protocol optimisation can be time-consuming
Colorimetric Assay for acid hydrolysate of chitin	• Detects decomposition product of chitin after acid hydrolysis	• Low cost • Quantitative • Simple protocol	• Destructive • Cannot distinguish forms of chitin • Spatial information is lost
Calcofluor-white	• Visualises chitin in relation to cells and tissues	• Non-destructive to tissues and cells • Low cost • Commercially available	• Also binds to cellulose • Also binds to N-acetyl-D-glucosamine and sialic acid
Wheat-germ agglutinin (WGA)			
Chitin-binding domain fused with green fluorescent protein (CBD-GFP)		• Non-destructive to tissues and cells • Specific to chitin	• Requires a time-consuming bioengineering approach to express and purify CBD-GFP

1479

1480

4. Cellular biomineralization mechanisms (cont.)			
Technique	**Measurement(s)**	**Advantages**	**Disadvantages**
OMICS – transcriptomics	• mRNA of expressed genes	• Assesses the molecular pathways of the organism from expressed genes or proteins • Provides a whole physiological picture	• mRNA presence may not represent protein activities • Tissue-specific response • Costly • Identification of transcripts in a non-model marine species is difficult
OMICS – proteomics	• Total protein profile		• Shell proteins occurring at low quantity of 5% • High-sensitivity method like iTRAQ is very costly

			• Identification of protein in a non-model marine species is difficult
Cellular pH imaging	• *Intracellular pH indicated by a pH sensitive ratiometric probe* • *Visualises the sites of biomineralisation*	• *Examines living organisms* • *High spatial resolution*	• *Not well established and optimisation* • *Ratiometric pH probes require calibration*
Physiological inhibitors and stimulators	• *Enables examination of the physiological response of a non-model organism* • *The importance of a biological pathway is evaluated by a specific inhibitor*	• *Applies to non-model organisms*	• *Some inhibitors are not specific to a single pathway* • *Action of inhibitors should be verified by a known physiological measurement*

1481

1482